Preparation, Optimization, and Characterization of Mirtazapine-loaded NLCs based Hydrogel for the Treatment of Pruritus

M.Phil Thesis

by

MUHAMMAD AKHTAR

Department of Pharmacy
Faculty of Biological Sciences
Quaid-i-Azam University
Islamabad, Pakistan
2023

Preparation, optimization, and Characterization of Mirtazapine-loaded NLCs based hydrogel for the Treatment of Pruritus

Thesis Submitted by

MUHAMMAD AKHTAR

Registration No. 023332111010

to

Department of Pharmacy,

In Partial Fulfillment of the Requirements for the Degree of

Master of Philosophy

in

Pharmacy (Pharmaceutics)

Department of Pharmacy
Faculty of Biological Sciences
Quaid-i-Azam University
Islamabad, Pakistan

2023

AUTHOR'S DECLARATION

I Muhammad Akhtar hereby declare that the thesis entitled "**Preparation, optimization, and characterization of Mirtazapine-loaded NLCs based hydrogel for the treatment of Pruritus**" submitted at Department of Pharmacy, Faculty of Biological Sciences, Quaid-i-Azam University Islamabad for the award of degree of Master of Philosophy in Pharmacy (Pharmaceutics) is the result of research work carried out by me under the supervision of Dr. Ahmad Khan during the period 2021-2023. I further declare that the results present in this thesis have not been submitted for the award of any other degree or fellowship and I am aware of the terms copyright and plagiarism, and I will be responsible for any copyright violation found in this work.

_____

MUHAMMAD AKHTAR

Date: _____

PLAGIARISM UNDERTAKING

I, **Muhmmad Akhtar**, solemnly declare that research work presented in the thesis titled "**Preparation, optimization, and characterization of Mirtazapine-loaded NLCs based hydrogel for the treatment of Pruritus**" is solely my research work with no significant contribution from any other person. Small contribution/help wherever taken has been duly acknowledged and that complete thesis has been written by me.

I understand zero tolerance policy of Quaid-i-Azam University, Islamabad, and HEC towards plagiarism. Therefore, I as an author of the above titled dissertation declare that no portion of my thesis is plagiarized, and every material used as reference is properly referred/cited.

I undertake that if I am found guilty of committing any formal plagiarism in the above titled thesis even after award of M.Phil Degree, the University reserves the right to withdraw/revoke my M. Phil degree and that HEC and University has the right to publish my name on the HEC/University website on which names of those students are placed who submitted plagiarized thesis.

_____

MUHAMMAD AKHTAR

APPROVAL CERTIFICATE

This is certified that the dissertation titled "**Preparation, optimization, and characterization of Mirtazapine-loaded NLCs based hydrogel for the treatment of Pruritus**" submitted by **Mr. Muhmmad Akhtar** to the Department of Pharmacy, Faculty of Biological Sciences, Quaid-i-Azam University Islamabad, Pakistan is accepted in its present form as it is satisfying the dissertation requirements for the degree of Master of Philosophy in **Pharmacy (Pharmaceutics).**

Supervisor:

_____

Dr. Ahmad Khan
Associate professor
Department of Pharmacy
Quaid-i-Azam University
Islamabad, Pakistan.

External Examiner:

_____

Dr. Shahzad Hussain
Drugs Control and
Traditional Medicine Division,
National Institute of Health,
Islamabad.

Chairman:

_____

Prof. Dr. Ihsan-ul-Haq
Chairman
Department of Pharmacy
Quaid-i-Azam University
Islamabad, Pakistan.

Dated: _____

DEDICATION

I would like to show my gratitude and humbleness to ALLAH Almighty for his countless benediction upon me, without his blessing I would never be able to accomplish anything in my life.

Then, I dedicate my work to PROPHET (S.A.W.W)

and

To my Father, Mother, Teachers, Siblings and Friends,

They always guide and give me the courage to accomplish my dreams. Thank you for giving me the courage and constant support.

Thank you for showing me the right way, and teaching me to hope in ALLAH Almighty. May Allah give you the best reward.

TABLE OF CONTENTS

Acknowledgments

All the praises and thanks to **Almighty ALLAH,** who bestowed His innumerable blessings upon humankind, one of which is knowledge distinction for humankind. He has opened every impossible pathway for me, and I am forever His indebted slave. I offer my gratitude to the **Holy Prophet Muhammad (PBUH)** who preached to us to seek knowledge for the betterment of humankind.

At this moment of accomplishment, first of all, I pay homage to my worthy supervisor **Dr. Ahmed khan**. This work would not have been possible without his guidance, support, and encouragement. I am grateful to be under his umbrella of education for this tenure. He is not only an excellent mentor but also a very kind human being. Thank you for being with me patiently during all phases of this dissertation.

I am extremely indebted to **Prof**. **Dr. Ihsan-ul-Haq** (Chairman) for providing the necessary resources to accomplish my research work.

I am indebted to my all my seniors especially Muhammad Usman, Abeer Tariq and colleagues Ahmed Abdur Rahman, Muzammil Ilyas, Aqeedat Javaid, Syed Baqir Raza Naqvi, Shakeel Abbas and Nimra Hameed for providing a stimulating and fun filled environment and many rounds of discussions in lab(s) with them helped me a lot.

Finally, I am so much grateful of my family, especially my brother for his unconditional love has always been my greatest strength and reason for success. It is only because of my family support and cooperation that make me able to complete my degree.

MUHAMMAD AKHTAR

List of Tables

List of Figures

List of Abbreviations

Abbreviations	Description
DMF	Dimethyl formamide
DMSO	Dimethyl sulfoxide
DSC	Diffraction scanning calorimetry
EE	Entrapment efficiency
FTIR	Fourier transform infrared microscopy
MRT	Mirtazapine
MV	Millivolt
NLCs	Nanostructure lipid carriers
PBS	Phosphate buffer saline
PDI	Polydispersity index
PS	Particle size
SEM	Scanning electron microscopy
SLNs	Solid lipid nanoparticles
XRD	X ray diffraction
XRD	X ray diffraction
Z P	Zeta potential

Abstract

Pruritus is poorly localized, non-adapting with the unpleasant sensation that provokes a desire to scratch. The most common dermatological disorder is pruritus and itching are a painful sign of this disease. Due to itching patients scratch the skin which causes more irritation and thus leads to the formation of pruritus. To address the side effect issues linked with its systemic delivery, a NLCs loaded MRT was prepared by microemulsion method and incorporate into the gel for more consistency for its topical delivery in treatment pruritus patients. The formulation was optimized in terms of particle size zeta potential, polydispersity index (PDI), and entrapment efficiency by keeping in view the amounts of drug tween 80 and Lipids ratio. Optimized nano formulation exhibited the particle size of 186.3 nm, with 0.217 PDI, zeta potential of -26 mV and entrapment efficiency 86.3%. MRT was computed through UV spectroscopy at wavelength of 230 nm. FTIR analysis confirmed the compatibility of nano formulation's components. DSC study showed the successful encapsulation of drug inside lipid matrix of nano formulation Further, the gel-based optimized mirtazapine-loaded NLCs dispersion was analyzed for rheology and textural characterization. l. Prepared liposomal gel had a transparent appearance, non-gritty texture, pH and spreadability of 322.33± 0.25%² respectively. Nano formulation loaded gel exhibited a drug release of 71.92% in 24 hours and followed Korsmeyer- Peppas model. Ex vivo skin permeation depicted only 6.20 µg/cm² drug permeation across the skin after 24 hours. Skin irritation study showed no signs of erythema and edema in nano formulation treated group. Stability study showed that the nano formulation is sTable for a period up to three months. Thus, MRT loaded NLCs gel was successfully prepared and can act as a promising vehicle for topical delivery in pruritus.

CHAPTER 1

INTRODUCTION

1. INTRODUCTION

1.1. Background

According to a review article, pruritus is defined as “poorly localized, non-adapting with the unpleasant sensation that provokes a desire to scratch (Weisshaar *et al.*, 2003). The most common dermatological disorder is pruritus and itching is a painful sign of this disease. A sense of itching provokes the desire to scratch the skin. Due to itching patients scratch the skin which causes more irritation and thus leads to the formation of pruritus. Bernhard described the term itching as: "Itching is a sensation that, if severe enough, causes either intentional or reflex scratching or the urge to scratch” (Bernhard, 2005). It was reported in a study that 85% of patients experience itching in pruritus (Prignano *et al.*, 2009). Server pruritus may cause suicidal temptation, due to its psychological implications as shown in Figure 1.1 (Prignano *et al.*, 2009).

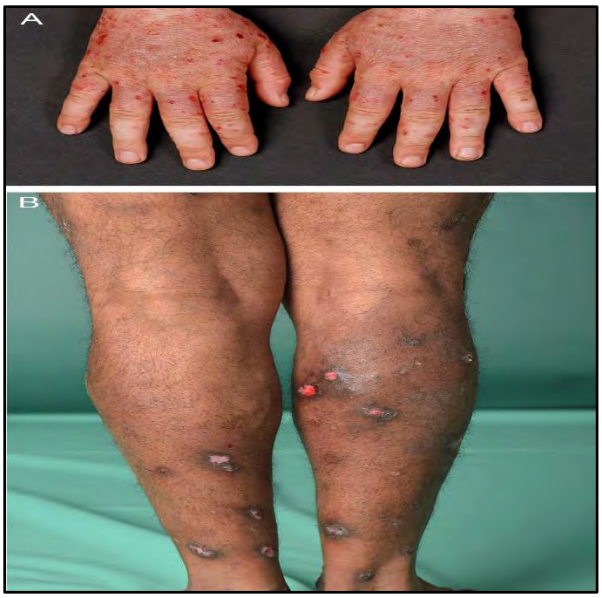

Figure 1.1. Scratching lesion in chronic pruritus.
Note: *A: Showing atopic dermatitis B: showing diabetogenic pruritus* (Pereira and Ständer, 2017).

1.2. Epidemiology

The most common acute and chronic skin diseases cause itching of the skin. In pruritus, itching is a major sign of the disease. About 23 to 44 million American people are suffering from chronic pruritus, whether it is a cutaneous or systemic condition (Mollanazar *et al.*,

2015). In the point prevalence study, it was proved that 8.2% of individual was found to be affected by pruritus (Metz and Ständer, 2010).

1.3. Classification of Pruritus

According to the International Forum for the Study of Itch (IFSI) into six categories, mostly acute and chronic pruritus. chronic pruritus further divided into three major groups based on clinical manifestation (Ständer *et al.*, 2007)

- Group I
- Group II
- Group III

1.3.1. Group I

This type of individual typically has unhealthy or irritated skin. As a result, the skin lesions present in people with this condition are caused by the underlying disease.Several dermatological disorders are associated with pruritus such as infectious dermatoses, inflammatory dermatoses, autoimmune dermatoses, dermatoses of pregnancy, neoplasms, and some drug reactions (Ständer *et al.*, 2007).

1.3.2. Group II

In this group patient have pruritus on primarily normal and non-inflamed skin, having second scratch lesion. These lesions arise due to scratching if the skin. This type of pruritus due to systemic disease, lymphoproliferative diseases, hematological, visceral neoplasms, pregnancy neurological disorder, somatoform/ psychogenic diseases, and drug associated reactions (Ständer *et al.*, 2007).

1.3.3. Group III

In this group, severe secondary chronic scratch lesions cause pruritus. In chronic pruritis patients extensively scratch the skin which in turn damages the skin and leads to excoriations, crusts, papules, lichenification, and nodules formation. When the lesion is recovered leaves scars on the skin as a result of hyperpigmentation or hypopigmentation. The size of the lesion is the variable size at different stages. The root cause may be skin-

related, systemic, nerve-related, or physical or psychological ailments (Ständer *et al.*, 2007).

Based on the origin chronic type of this disease have further six categories (Ständer *et al.*, 2007).

I) Pruritoceptive/cutaneous/dermatological pruritus,
II) Systemic pruritus,
III) Neurological pruritus (includes neuropathic and neurogenic),
IV) Somatoform/psychogenic pruritus,
V) Mixed
VI) Others

These categories are helping the physician to properly diagnose and prescribe better treatment interventions. A brief explanation of these type is given below.

1.3.4. Pruritoceptive/cutaneous/dermatological pruritus

Originates from skin conditions caused by the activation of specialized C-fiber free nerve sensory endings due to pruritogens. The main cause of this type of itch are dryness, inflammation, and skin damage.

1.3.5. Systemic pruritus

Emerges from a disease affecting the organ rather than the skin. For example, endocrine diseases, metabolic, liver, infectious, hematological, lymphomas, visceral neoplasms, and drug related diseases.

1.3.6. Neurological pruritus

Develops due to illnesses or disorders in the central or peripheral systems, such as nerve damage, compression, or irritation. Neurological pruritus encompasses both neuropathic and neurogenic pruritus. Neuropathic pruritus arises from damage to the nervous system anywhere along the afferent pathway.

1.3.7. Somatoform/psychogenic pruritus

This type of pruritus develops alongside psychosomatic and psychiatric disorders such as scratching brought on by depressive disorders, hallucinations, eating disorders, obsessive-compulsive disorders, anxiety disorders, delusional parasitosis, schizophrenia, and exhaustion. Mixed

Emerges due to the presence of multiple underlying reasons or diseases. For example, pruritus occurs in conjunction with chronic renal failure (uremia).

1.3.8. Other's pruritus

This type has an unknown underlying cause and have undetermined origin.

Different classification of pruritus is shown in Figure 1.2.

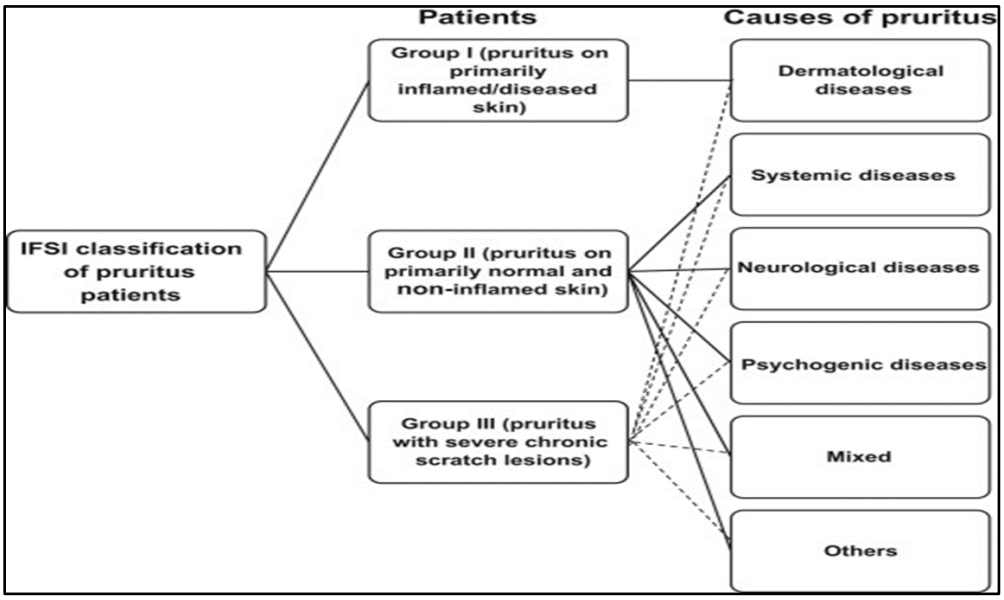

Figure 1.2. IFSI classifications of pruritus (Reich *et al.*, 2011, Ständer *et al.*, 2007).

1.4. Pathogenesis and Mechanism

Different physical and chemical factors are involved in the pathogenesis of pruritus and its mechanism are described below.

1.4.1. Physical stimuli and neural pathways

Many physical stimuli, like as light touch, pressure, vibration, and wool, as well as thermal and electrical stimuli, like transcutaneous or direct nerve stimulation, can make somebody itch. Free nerve terminals in the skin detect itching, and unmyelinated C fibers and myelinated A neurons in the skin transmit those feelings to the brain central spinothalamic tracts (Ständer *et al.*, 2007a). Research using microneurography has shown that the pathways responsible for transmitting itch and pain are distinct (Ständer *et al.*, 2003).

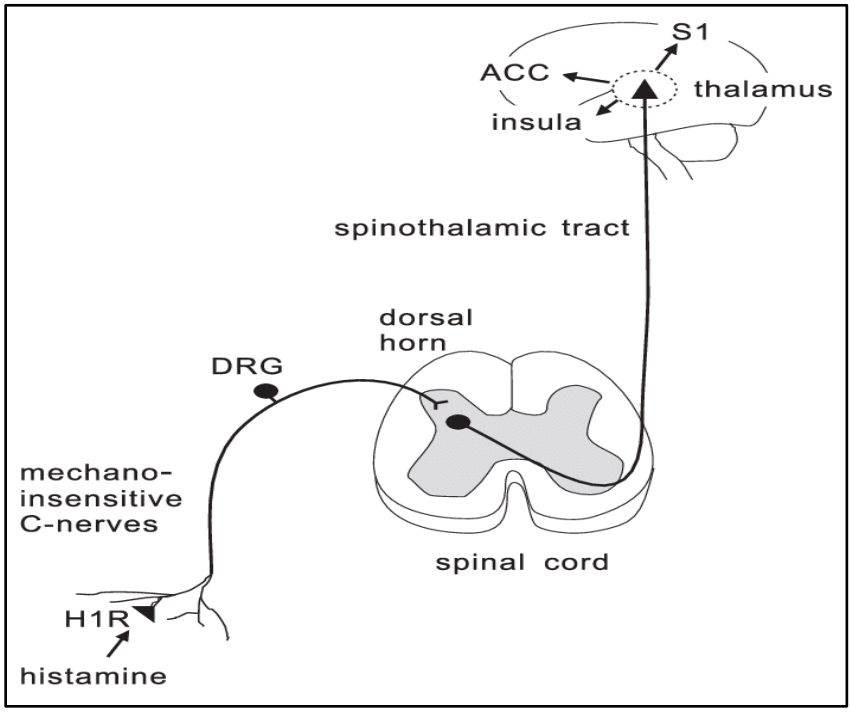

Figure 1.3. Neural pathway of itch (Ikoma, 2009).

1.4.2. Chemical mediators

Histamine plays a major role in causing itching, although other chemicals can also contribute to the sensation. Some of these chemicals, like neuropeptides, cause itching by activating histamine in mast cells and can be treated with antihistamines (Ständer *et al.*, 2003). However, some chemicals work independently and cannot be treated with antihistamines, making them ineffective for certain types of itching. Opioids have a dual effect on itching, both through their central action in the brain and by increasing histamine-induced itching in the periphery.

1.4.3. Central mechanism

People who have tumors or lesions affecting the central nervous system have been found to experience persistent itching (Taylor *et al.*, 2010). Additionally, the use of opioids during epidural anesthesia has been known to cause itching.

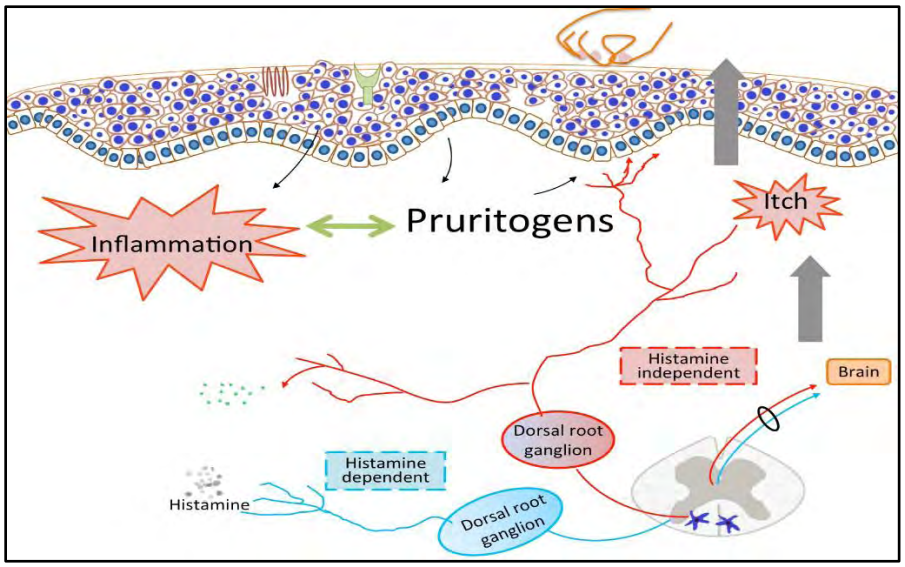

Figure 1.4. Pathogenesis of pruritis (Wong *et al.*, 2021).

1.5. Etiology

Itching can be caused by both skin-related and systemic issues, and it is crucial to determine if there is any skin rash present. The presence of a characteristic rash typically confirms a primary skin disorder. Itching is a common symptom of many skin illnesses, such as atopic eczema, dermatitis herpetiformis, lichen simplex chronicus, and nodular prurigo. Without it, the condition cannot be recognized. Mild urticaria or aquagenic pruritus, in which histamine levels are high enough to elicit a sensory response but not a skin reaction, and hence no apparent skin findings. Before the typical blisters develop, bullous pemphigoid might start with a prebullous itching phase that can last months (Alonso-Llamazares *et al.*, 1998).

In some cases, mycosis fungoides can present as itching without a visible rash, and is only diagnosed through a biopsy (Taylor *et al.*, 2010). It's critical to establish whether the irritation started before the skin eruption. When people scratch themselves excessively, it can result in secondary skin conditions such excoriation, lichenification, dryness,

eczematization, and infection. Over-bathing and skin irritation from topical treatments can also result in dermatitis. These symptoms should not be mistaken for the primary skin disorder, as some conditions can be serious, and it is risky to simply label general itching as "nonspecific eczema" without first excluding other possible causes. Itching caused by systemic diseases is usually widespread and may be the only symptom, with no specific rash present. Chronic itching can also be associated with neurological and psychiatric conditions.

1.6. Skin

The largest and most protective organ in the human body is the skin. It protects the body from the harsh environment, maintained homeostasis, acts as a sensory organ that regulates the body temperature, and prevents water loss. It protects the body from harmful UV radiation and site for vitamin D synthesis. Its characteristics depend on the location and thickness of the skin.

1.6.1. Anatomy of skin

The skin consists of three main layers and different cell

1. Epidermis,
2. Dermis
3. Subcutaneous tissue (hypodermis)

1.6.1.1. Epidermis

The epidermis, made up primarily of keratinocytes, is a constantly evolving multilayered tissue that can self-renew. The keratinocytes can alter their structure and composition through differentiation, which results in the production and presentation of different structural proteins and lipids. This makes them crucial for the proper functioning of the skin (Savoji *et al.*, 2018). Further division of the epidermis is given below

a) Stratum germinativum
b) Stratum corneum
c) Stratum granulosum
d) Stratum lucidum (only in some parts)

e) Stratum spinosum

1.6.1.2. Dermis

The dermis, which is approximately 1 to 2 millimeters in thickness, acts as a support system for the skin and contributes to its elasticity due to its abundant elastin content. This layer is made up of two parts: a loosely structured upper papillary layer of collagen fibers and a denser reticular layer of collagen fibers (Savoji *et al.*, 2018).

1.6.1.3. Hypodermis

The hypodermis, the lowest sublayer of the skin, serves as a cushion to absorb shocks and insulates the body from heat. It primarily consists of fibroblasts and adipocytes (Savoji *et al.*, 2018).

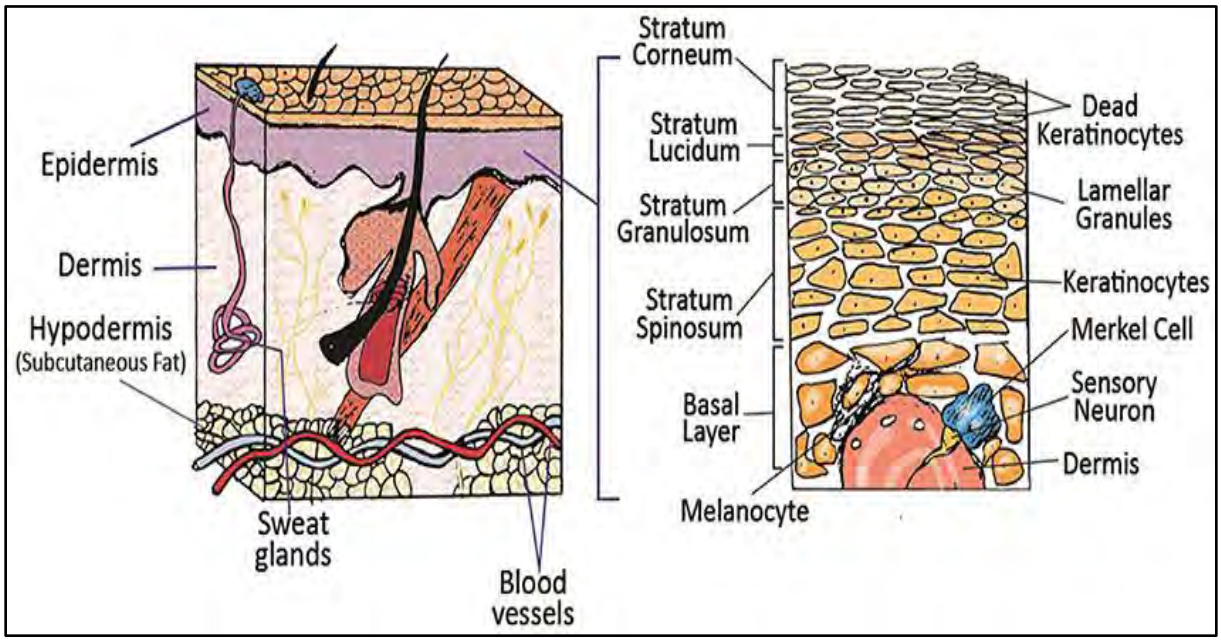

Figure 1.5. Skin anatomy (Savoji *et al.*, 2018).

1.7. Treatment Strategies for Pruritus

Different treatment, strategies are involved in treating pruritus by repairing the barrier functions

1.7.1. Topical treatment of pruritus

1. Moisturizers
2. Emollients
3. Barrier repair creams
4. Topical calcineurin inhibitors (Doxepin)
5. Local anesthetics
6. Salicylic acid 2-6%
7. Capsaicin cream
8. Menthol
9. Topical steroids
10. Topical Immunomodulators (Patel and Yosipovitch, 2010)

1.7.2. Systemic medications for pruritus

1. Opioid's receptor agonist/antagonist (according to the type of receptor)
2. Neuroleptic
3. Immunosuppressant
4. Substance p antagonist
5. Oral antihistamines (except for urticaria, antihistamines are not effective for conditions causing itching.) (Patel and Yosipovitch, 2010)
6. Selective norepinephrine reuptake inhibitor (SNRI) (Patel and Yosipovitch, 2010)

1.7.3. Possible Future Treatments for Pruritus

1. Methylnaltrexone
2. NGX-4010
3. TS-022
4. Serine proteases/PAR2 antagonists
5. IL-31 antibody (Patel and Yosipovitch, 2010)

1.8. Mirtazapine

Mirtazapine works as an antagonist at following receptors

1. Noradrenergic α2 receptors

2. Serotonin receptors (5-HT2 and 5-HT3)
3. 5-ht1 serotonergic neurotransmission (De Boer, 1995)

Mirtazapine is involved in boosting central noradrenergic. Its antipruritic effect has been reported by multiple researchers after oral administration (once daily at doses of 7.5 mg, 10 mg, or 15 mg) due to its high affinity for central and peripheral H1 receptors, which helps to inhibit histamine, the main mediator of itching (Stimmel *et al.*, 1997). Mirtazapine has been shown to relieve itching in patients with leukemia, lymphoma (including cutaneous lymphoma), cancer, chronic kidney disease, atopic dermatitis, and cholestasis (Patel and Yosipovitch, 2010).

1.8.1. Mechanism of action of Mirtazapine as an antipruritic

The most common itch-inducing chemical is histamine, and this antidepressant (Mirtazapine) mainly blocks H1 and H2 histamine receptors. The imidazole ring is joined to the primary amino group (-NH2) by two methylene groups as well as a hydrophilic histamine molecule. Histamine's antagonists, such diphenhydramine, loratadine chlorpheniramine, and chlorcyclizine, have a tertiary amino group and have the same general formula, in contrast to histamine itself, and hence exhibit antihistaminic activity. The secondary and tertiary amino groups in the general chemical structure of antidepressants may elucidate their antihistaminic activity, which is correlated to their structure-activity with antihistaminic.

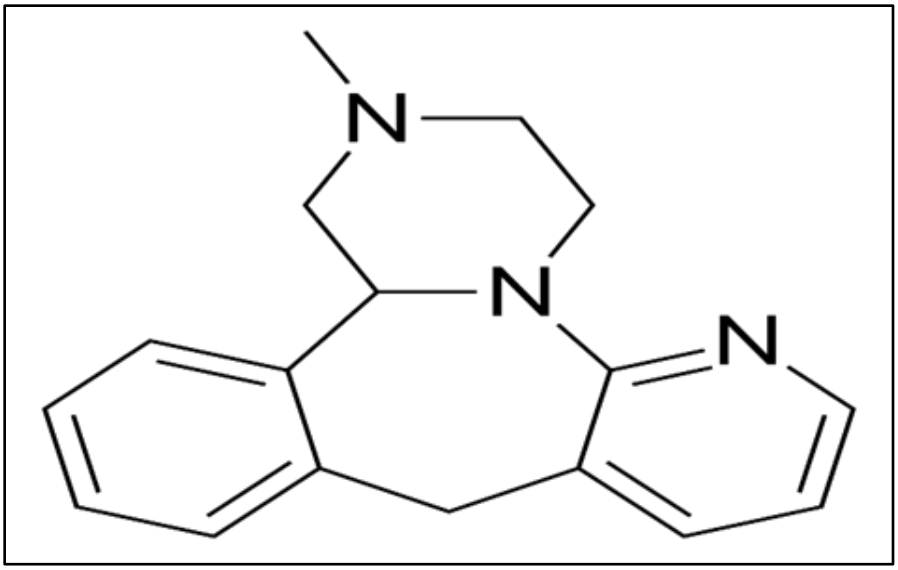

Figure 1.6. Structure of mirtazapine.

1.8.2. Properties of mirtazapine

Mirtazapine's various characteristics are described in Table 1.1.

Table 1.1. Properties of mirtazapine

Properties	
IUPAC Name	1,2,3,4,10,14b-hexahydro-2- methyl pyrazino[2,1-a]pyrido[2,3-c]benzazepine
Molecular weight	265.35 g/mol
Molecular formula	C17H19N3
Solubility	Freely soluble in methanol and chloroform, insoluble in water
Log P	2.7
Half life	20 to 40 hours
Dose	7.5 mg, 15 mg, and 30 mg
Melting point	114-116 ◦C

1.9. Topical Drug Delivery System

Topical administration, due to its simplicity and cost-effectiveness, is the chosen method of delivering medicinal substances locally. The challenge in developing a therapeutic system is to maintain an optimal concentration of the medicine at the site of action for a sufficient amount of time. In recent years, topical administration has gained significant attention. However, conventional topical medication delivery methods have limitations, such as low retention and bioavailability. Effective topical delivery product formulation requires the manipulation of protective barriers and the selection of a soluble medication carrier. Further research is needed to improve topical drug delivery systems, either by

enhancing their efficacy or reducing side effects compared to current patented techniques. This route of administration can perform the following functions

1. Reduction in the need for systemic administration of drugs
2. Reduction in the dose
3. Decreased unintended ADR’s

1.9.1. Barriers in topical drug delivery

The skin serves as a physical barrier, primarily composed of the stratum corneum, which makes it a key focus for topical drug delivery. The various components of the skin, such as the stratum corneum, epidermis, dermis, and appendages, have properties that can either limit or decrease the penetration of topical products. Other factors that pose challenges and cause difficulties in topical drug delivery include:

1.9.2. Factors related to skin

1. Skin heterogeneity in metabolism and turnover
2. Variability in percutaneous absorption due to disease state and age
3. Stratum corneum
4. Viable epidermis
5. Skin's reservoir capacity

1.9.3. Drug related factors

1. Drug vehicle's physicochemical characteristics
2. Drug's irrational potential and toxicities
3. Drug's physicochemical characteristics
4. Dosing conditions

1.9.4. Strategies to improve the topical absorption

Above mention barrier related problems to create the urge among scientist to investigate the method that improves the absorption of topical drugs by improving barrier functions. Different strategies are given below

1. Physical barrier enhancer (compromise the skin's barrier function)
2. Chemical based enhancer (increase the penetration of topical drugs)

a) Pyrrolidone
b) Amines
c) Surfactant
d) Alcohols
e) Polyalcohol
f) Phospholipids

1.10. Mechanisms Behind Improved Absorption

1. Turning the lipids into a more fluid state and breaking down the crystalline structures
2. Disrupting the highly organized structure of the stratum corneum
3. Breaking down the keratin or lipid components in the stratum corneum

Chemical based enhancers may irritate the skin that's why have limited use. That's why the focus of research has shifted to nanotechnology, specifically nanoparticles as a potential alternative for delivering drugs through topical applications. Nanolipid carriers, for instance, are widely used for delivering both hydrophobic and hydrophilic molecules with a regulated release over time.

1.11. Nanostructure Lipid Carrier

Lipid formulations like Nano Lipid Carriers (NLCs) require incorporating a variety of products. The bioavailability and solubility of insoluble drugs are the two main factors that can be improved through formulations like NLCs. There are several techniques and methods for preparing or formulating NLCs, such as high-pressure homogenization. NLCs are a novel type of drug delivery system and formulation that offers improved stability and loading, and the ability to create concentrated dispersions.

1.11.1. Structure of NLC's

When it comes to solid lipid nanoparticles, the matrix creates a near-perfect crystal lattice structure, providing limited space for accommodating active components. The supposed

inner core structure of SLNs is depicted in Figure 1.7. Another way of producing crystals is to employ a combination of solid and liquid lipids. Defects in the particle matrix offer more space for drug molecules to gather in non-crystalline clusters (amorphous clusters).

1.11.2. Types of NLC's

The production of NLCs can be carried out through various methods, depending on the forming technique and the composition of the lipid mixture, to increase the payload of active compounds and reduce drug loss during storage. The three types of NLCs are as follows

1. The imperfect type, and
2. The amorphous type.
3. The multiple types

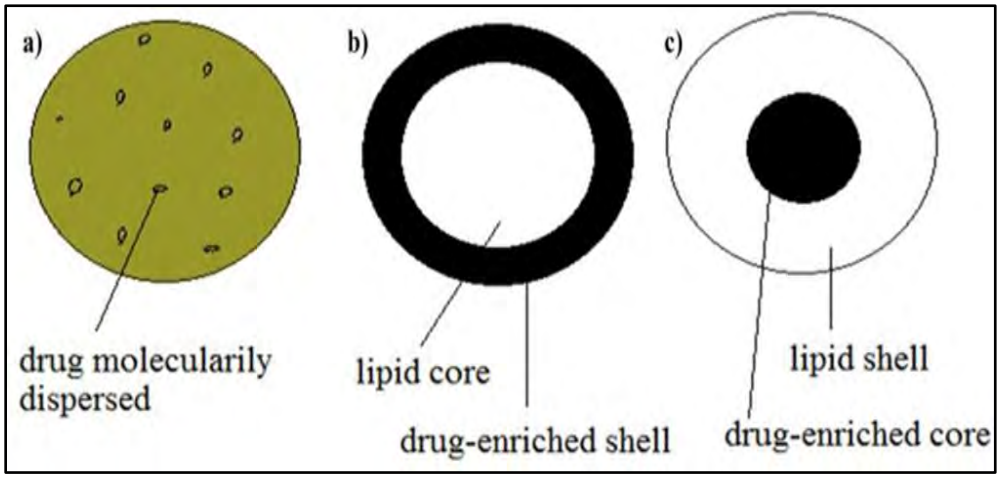

Figure 1.7. Different models of SLNs.
Note: *a) solid solution model, b) core-shell model (drug-enriched Shell), c) core-shell model (drug-enriched core)*

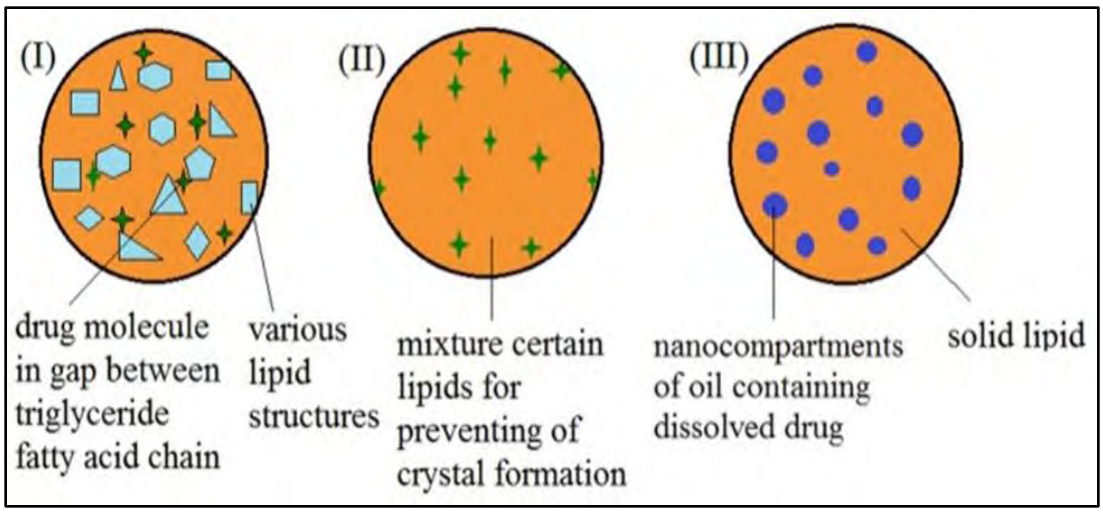

Figure 1.8. Based on class different structure of NLC.
Note: Class I (imperfect type), class II (formless type), and class III (multiple types). To prevent drawbacks of SLN, the NLC should possess sufficient gaps to better drug accommodation

1.11.3. Advantages of NLC's

The following are some of the benefits of NLCs:

1. Improved physical stability and easy preparation and scaling
2. Enhanced dispersibility in aqueous media
3. Increased skin occlusion
4. Extended drug release
5. High entrapment of both lipophilic and hydrophilic drugs, with controlled particle size
6. Small lipid particle size that allows for close contact with the stratum corneum, leading to increased drug permeation into the skin
7. Improved skin hydration and elasticity, and a favorable benefit-to-risk ratio due to their solid lipid matrix
8. Regarded as efficient and generally considered safe or have regulatory approval
9. Development of an innovative and efficient carrier system for lipophilic chemicals

1.11.4. Methods of preparation of NLC’s

Various methods are available for the preparation of NLC’s

1. Solvent emulsification/evaporation technique

2. High pressure homogenization (HPH)

a) Hot high-pressure homogenization

b) Cool high-pressure homogenization

3. Micro-emulsion formation method
4. Ultrasonic solvent emulsification technique

1.11.5. Mechanism of skin penetration and drug release in NLCS

The rate of drug release is influenced by several factors which includes

1. Desorption,
2. Diffusion, and
3. Solubility of the drug within the nanoparticle matrix,
4. Erosion, degradation, and a combination of these processes.

The release mechanism is controlled by the biodegradation of matrix components, diffusion, and solubility, and can be triggered by an impulse during particle administration. NLCs have a disordered lipid structure, allowing for higher drug loading. This disarranged structure can activate certain release processes. The aim is to have a solid lipid matrix with a less organized structure for high drug loading (Jaiswal *et al.*, 2016).

1.12. Problem Statement

The low solubility of drugs belonging to BCS class II in water, combined with intense metabolism during the first pass leads to low bioavailability of only 50%. This requires higher dosages to be administered, which in turn can cause side effects such as dry mouth, sedation, and stimulation of appetite.

1.13. Rationale

The main purpose of the current study is to provide the topical route and an alternative route. To provide a sustained-release drug that increases the duration of action and hence improves the therapeutic efficacy. Moreover, higher drug loaded capacity of the NLC's formulations can minimize the leakage of the drug during the storage.

1.14. Aim and Objectives

1.14.1. Aim

The main objective of this study was to evaluate the potential of Mirtazapine-loaded nanostructured lipid carriers (MRT-NLCs) as a topical delivery system.

1.14.2. Objectives

1. . MRT- loaded Nanostructured Lipid preparation, optimization, and characterization
2. Development of MRT-loaded gel and characterization of mirtazapine loaded Nanostructure lipid carrier gel.
3. In-vitro release and ex-vivo evaluation of developed MRT-loaded NLCs gel Carriers.

CHAPTER 2

MATERIALS AND METHODS

2. MATERIALS AND METHODS

2.1. Chemicals

Mirtazapine (active drug) was kindly gifted by Global Pharma Pvt limited, Compritol was obtained from Gattefosse France and gifted by Morgan chemicals, Tween 80, Oleic Acid, Chitosan MW 310000-375000 (Sigma Aldrich cas-9012-76-4), Methanol(Sigma Aldrich), dipotassium hydrogen phosphate (Scharlau, Germany)Glutaraldehyde, Acetic Acid, sodium dihydrogen phosphate (Scharlau, Germany), formaldehyde,, Potassium dihydrogen phosphate (Scharlau, Germany), Sodium chloride (Merck, Scharlau, Germany), Sodium hydroxide (Merck, Scharlau, HOHENBRUNN, Germany), Nutrient Broth (Merck, Germany), Distilled water was used from Pharmaceutics lab (Department of Pharmacy, QAU, Islamabad).

2.2. Apparatus

Weighing balance (RADEAG UK Ltd), Multi hot plate stirrer (MAGIK MG-855), Homogenizer (D-91126,Heidolph, Germany) Lyophilizer (Alpha 1-2 LD plus, CHRIST, Germany, Centrifuge machine (HERMLE LABORTECHNIK, Z-326K, Germany), Sonicator (Elma E-60 H Elmasonic), FTIR spectrophotometer, Dialysis membrane (Cell Sep®, T4 Series, Texas, US), Pharmaceutical Refrigerator (MPR-161D H, Panasonic, Japan), Freezer (Panasonic, Japan), pH Meter (EUTECH INSTRUMENTS pH 700), UV visible spectrophotometer (T80+ model PG instruments Limited, UK), Conical flasks, Funnel, Petri plates, Beakers, Micro Pipette, Micro filters, Syringes, Eppendorf tubes, Glass slides, Graduated cylinder, volumetric flasks Magnetic stirrer,(PERKIN ELMER), Water bath and Shaker (Memmert, WNB-7, Germany, Oven (Memmert, Germany), Zetasizer (Malvern instruments, Worcestershire, UK),Incubator, Laminar flow hood, Autoclave Machine, Transmission electron microscope, Viscometer, Distillation apparatus (Irmeco, GmbH IM50,Germany).

2.3. Animals

Male Sprague Dawley rats were purchased from NIH Islamabad, Pakistan and were used in anti-pruritic study. The animals were kept in animal house with proper bedding and care along with standard animal food and drinking water facility. Temperature and relative

humidity were maintained at 24-25°C and 50-60% respectively. The animal welfare act of NIH policy was utilized to guide the protocols used for animal studies, which were approved by the BIO ethics committee of Quaid-i-Azam University.

2.4. Preparation of MRT-Loaded NLCs

The Micro-emulsion method, with minor modifications, was used to develop MRT NLCs. In this process Lipid phase comprising Compitrol ATO 888, Oleic Acid, and drug (MRT) was heated to 85 ° C. Meanwhile, on hot plat, an aqueous phase containing surfactant (Tween 80) was heated to the same temperature. Both phases were heated for 30 seconds. Following that, the aqueous phase was progressively dispersed in the melting lipid phase and blended for 30 minutes with a magnetic stirrer at 800 rpm. The microemulsion then transferred to homogenization at 10,000 rpm for 15 mints. Finally, the resulting O/W micro emulsion was dispersed in ice cold water (2-3 c) in the ratio of 1:9 (nano-emulsion: water) MRT loaded NLCs (Moulik *et al.*, 1998).

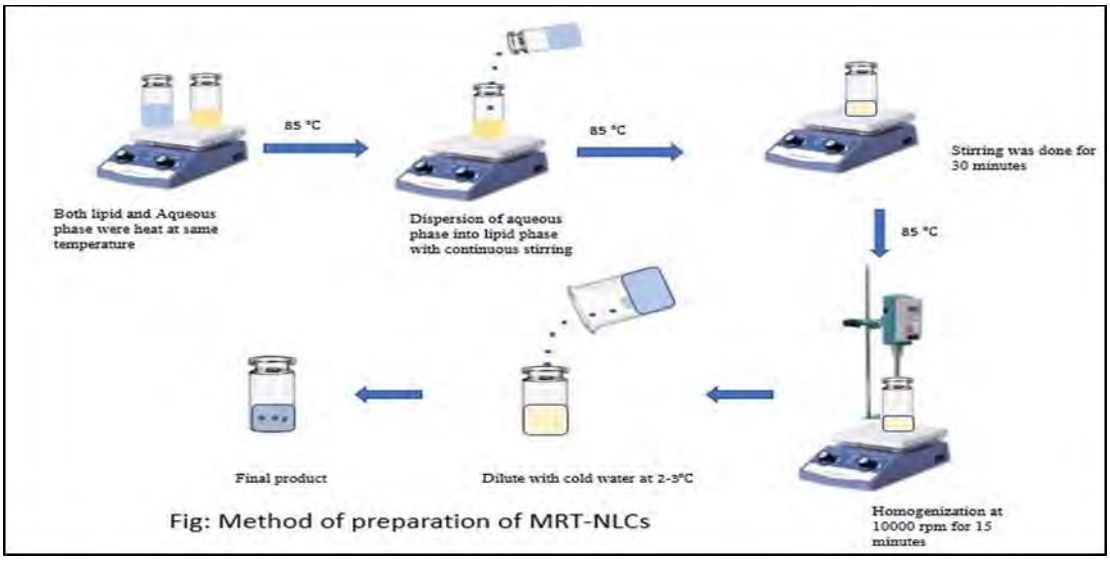

Figure 2.1. Process for preparing the MRT NLCs.

2.5. Optimization of MRT-Loaded NLCs

In design expert version 12, the Box Behnken model was used to optimise MRT-loaded NLCs. The medication, surfactant, and solid lipid (Compitrol, oleic acid) concentrations were altered, and the effects on particle size, zeta potential, PDI, and% EE were evaluated.

2.6. Characterization of MRT-Loaded NLCs

Using a zeta sizer ZS90 equipped with a 635 nm He-Ne laser, the particle size, polydispersity index, and zeta potential of MRT-loaded NLCs were determined. At a constant light incidence angle of 90 degrees and a temperature of 25 degrees, all measurements were taken using software version 6.34. (Malvern Instruments, Worcestershire, UK). In order to adequately dilute the samples before analysis, 10 mL of MRT-loaded NLCs were dissolved in 1 mL of distilled water, followed by 1 minute of vertexing the samples (Bhaskar *et al.*, 2009).(Sanad *et al.*, 2010).

2.7. Preparation of Standard Curve in Methanol

Mirtazapine standard curve was prepared in methanol with the help of UV spectrophotometry and the linearity range was found to be between 10-50 ug/ml. First prepare the stock solution of drug then further dilution in linearity range. After the dilution analyzed by UV spectroscopy at 290 nm (Karaşen *et al.*, 2000).

2.7.1. Calibration curve at pH 5.5 and 7.4 (PBS)

The PBS based standard curve was constructed as mentioned above. The rationale of the pH-based calibration curve was to evaluate the release behavior of both drugs at different pH conditions.

2.8. Entrapment Efficiency of MRT-Loaded NLCs

the sample was prepared, and equal volume was poured into 2-ml Eppendorf's. It is than centrifuged at 13,000 rpm, for 2 hrs. The entrapped drugs were settled down at the bottom in the form of pellets and the supernatant was draw off without agitation. Specified quantity of supernatant was diluted in the solvent in which drug dissolved (Methanol) in the ratio of 1:10(1 ml of supernatant in 10 ml solvent). It is than observed for free drug using UV spectrophotometer at 290 nm ((Rashidi Nodeh *et al.*, 2016, Misal *et al.*, 2012)

$$\% \text{ Entrapment efficiency} = \frac{\mathrm{wt}-\mathrm{wf}}{wt} \times 100$$

Where, Wt = Total drug concentration

Wf=Free drug concentration.

2.9. Scanning Electron Microscopy of MRT-Loaded NLCs

A scanning electron microscope (SEM) (LEO-430 Cambridge and UK) was used to examine the shape and surface morphology of an MRT loaded NLCs. Excess water was allowed to dry at room temperature after one drop of sample was placed on a slide. The slide was bonded to an aluminum stub with double-coated adhesive tape, and the stubs were then coated with gold to a thickness of 200 to 500 A using a gold sputter module in a high vacuum evaporator under an argon atmosphere. Photographs were taken at various magnifications. (Sanad *et al.*, 2010).

2.10. Solid State Characterization

2.10.1. Fourier transform infrared spectroscopy (FTIR)

Because of the solid nature of the samples, FTIR absorption spectra of mirtazapine, mirtazapine-solid lipid physical mixes, and MRT loaded NLCs were acquired by scanning over a range of 500-4000 cm1 with a resolution of 4 cm1 utilising Perkin Elmer Co., Waltam, USA instrument. MRT and all excipients used in the formulation were tested for compatibility. assessed (Kumar *et al.*, 2014).

2.10.2. Differential scanning calorimetry (DSC)

The DSC thermogram was used for MRT, physical mixture and lyophilized NLCs. Samples weighing approximately 5 mg were hermetically sealed in aluminum pans and analyzed by DSC 822e (Mettler-Toledo International Inc., Columbus, OH, USA)(Liu *et al.*, 2010).

2.10.3. Powder X-ray diffractometry

XRD Analysis was performed to check the crystalline structure and amorphous behavior of MRT loaded NLCs. XRD assay of pure MRT, Compitrol ATO 888 and lyophilized MRT loaded NLCs were studied by powder X-ray diffractometer (JDX 3532 Jeol Japan). Samples were positioned on sample stage and scanned from 2h to 60h with an operating voltage of 40 kV and current 30 mA (Pradhan *et al.*, 2015).

2.11. Preparation of MRT-Loaded NLCs Gel

1% Glacial acetic acid solution in distilled water was prepared for preparation of chitosan gel. ha1% acetic acid solution, the 2% weighed amount of chitosan was added and mix carefully on a magnetic stirrer at 600 rpm. Following the swelling, the remaining chitosan in small portions was added and properly stirred until the entire weighted chitosan was added and a homogeneous mixture was achieved. In last add few drops of Glutaraldehyde as a cross linker and stirrer at high speed for 5 min. To remove air bubble from the gel, the prepared gel was kept at room temperature overnight before the application.

2.12. Characterization of MRT-Loaded NLCs Gel

1% Glacial acetic acid solution in distilled water was prepared for preparation of chitosan gel. ha1% acetic acid solution, the 2% weighed amount of chitosan was added and mix carefully on a magnetic stirrer at 600 rpm. Following the swelling, the remaining chitosan in small portions was added and properly stirred until the entire weighted chitosan was added and a homogeneous mixture was achieved. In last add few drops of Glutaraldehyde as a cross linker and stirrer at high speed for 5 min. In order to remove air bubble from the gel, the prepared gel was kept at room temperature overnight before the application (Thomas *et al.*, 2016).

2.12.1. Homogeneity test

The homogeneity of the gel was determined by visually inspecting it for visible particles, bubbles, and lumps. The gel's consistency was tested by compressing it between the thumb and index finger to verify that it was homogeneous or not (Ahad *et al.*, 2017).

2.12.2. Drug content

Methanol 10 ml was used to dissolve one gram of MRT-loaded NLCs gel. After that, the produced solution was sonicated and filtered. Following filtration, the drug content was determined using a UV spectrophotometer (Ahad *et al.*, 2017).

2.12.3. Spreadability study

Spreadbility measures the extent with which gel can applied readily and uniformly on the skin.it was calculated by taking two slides. One of the glass slides was marked with 1cm circle in middle.0.5 g of prepared gel was placed in the marked circle. The second slide place over the first slide. A weight of 500gm was placed over the upper slide for 5 mi. Weight was then removed after 5 min and increase in diameter was noted.

Following formula was used to measure Spreadability index

$$Si=d^2\times\frac{\pi}{4}$$

Where Si is the spreadability index and d is the diameter in (mm) of the spread area (Sabir *et al.*, 2019).

2.12.4. Measurement of pH

It was very important for topical application and measured by pH meter at normal temperature. An average of 3 readings was taken.

2.12.5. Rheological study

The gel's rheological properties were evaluated using a rheometer (Brookfield). The gel's behavior was determined by testing its viscosity at varied rpm and determining the link between viscosity and shear rate (Alves *et al.*, 2011).

2.13. *In Vitro* Release Studies

The optimized pure drug dispersion pure drug gel NLCs dispersion and MRT-loaded NLCs gel in vitro drug release profile was done in phosphate buffer pH 7.4 and pH 5.5 At 37± 0.5 °C, dialysis membrane was used on a Franz diffusion cell apparatus. A dialysis membrane saturated in TDW was placed between the donor and receptor compartments. A dialysis membrane was loaded with 0.5 mL/0.5 g of NLCs dispersion/NLCs gel, which equated to 2.5 mg of medication. To keep the receptor volume constant, 1 mL aliquots of samples were taken from the sampling arm at regular intervals and replaced with fresh medium. The samples were then spectrophotometrically examined at a maximum wavelength of 290 nm (Elmowafy *et al.*, 2017).

2.14. Drug Release kinetics

Zero order, first order, higuchi model and korseymeres-papas model were applied to determine the best fit model based on R^2 and n values.

2.14.1. Zero order kinetics

The type of model where drug release in independent of the initial conc is known as zero The equation used for this model is given below.

$$Qt = Q_{\circ} + K_{\circ}t$$

Whereas t =time, $k_{\circ}$=zero rate constant,

Qt = quantity of drug release after time t and $Q_{\circ}$= drug constant at zero time.

2.14.2. First order model

The model where drug release is dependent upon initial drug conc is known as first order release kinetic. The equation used for first order release data are shown below.

$$\text{Log } c = \log c_{\circ} - k1t/2.303$$

Where k1 is first order rate constant, C is % of drug remaining after time t and $C_{\circ}$ is drug constant at zero time.

2.14.3. Hixon crowell model

This model demonstrates how changing particle size and surface area can alter drug release patterns.

2.14.4. Higuchi model

According to Ficks law, the drug is released from the matrix system in this model.

The data should be plotted which represent cumulative drug release versus square root of time.

$$Ft = Q = A$$

$$Ft = Q = Kh \times t1/2$$

Where Kh is Higuchi constant, Cs is the solubility of drug in matrix, A is the surface area, C is conc of drug at time zero, D is diffusion of drug from matrix, Q is the quantity if drug release.

2.14.5. Korsmeyer-peppas model

The kind of diffusion is determined by plotting data in the equation below using log time vs log percent drug release, the kormeyers model is used to determine the type of diffusion.

$Mt/M\infty = Kkp \times tn$

The diffusion exponent is n, the release constant is Kkp, the amount of drug released in time t is Mt/M.

2.15. Skin Permeation Study

Ex vivo permeability study Skin permeation study was carried out ex vivo in order to test the efficacy of the developed formulation by simulating skin conditions. For a period of 24 hours, the permeation profile of the MRT was investigated for MRT- loaded gel and MRT-loaded NLCs gel. Male Sprague Dawley rats were sacrificed and skin from the dorsal region was removed. Later it was shaved with a razor to carry out permeability study. For this purpose, the Franz-diffusion cell apparatus was used. The rat skin was mounted on the cells of the apparatus. Three different formulations were studied in a buffer media of pH 5.5. Formulations included 0.5 g of nano formulation loaded gel, 0.5 g drug loaded gel and 1 mL of nano formulation. Each of these formulations contained 1 mg of MRT. These weighed formulations were applied to the skin such that the upper layer of skin faced the donor compartment. Samples were taken at time intervals of 30 minutes, 1, 2, 4, 6, 8, 12 and 24 hours. After taking samples, same volume of buffer media was added in order to maintain sink conditions. The samples were analyzed using a UV spectrophotometer at wavelength 290 nm (Kaur *et al.*, 2020).

2.16. Skin Irritation Study

Skin irritation testing is done to look for any potential irritation induced by the developed formulation when applied topically male Sprague rats were taken, and their hair were removed using a razor. Rats were kept under observation for 24 hours in order to check any induced injury before the start of the study. The control group received no treatment or intervention. Intervention was made in case of negative control by applying 0.8% formalin solution only. One group was treated with the application of drug loaded gel and lastly fourth group was applied with nano formulation loaded gel. Erythema grading scale

was used to evaluate the extent of irritation in each group. Finally slides were prepared for histopathological study.

CHAPTER 3

RESULTS

3. RESULTS

3.1. Optimization of MRT-Loaded NLCs

A total thirteen runs were generated by Design Expert by varying the concentration of independent variable i.e., solid lipid, surfactants tween 80 and Drug. Software selects number 9 formulation as optimize on the basis of goal set of particle size, zeta potential, PDI and entrapment efficiency after data entered for each run. The optimize formulation has particle size is 186.3 nm and zeta potential -24.4 mev. Different factors affecting the MRT loaded gel are shown in Table 3.1.

Lipid ratio =9:1-7:3 % Tween ratio =0.2-0.5%
Number of Runs=13

Table 3.1. Different factors affecting the MRT loaded gel.

Run	Factor:1 Solid lipid	Factor:2 Tween 80	Factor:3 Drug	Response:1 Particle size	Response:2 Zeta potential	Response:3 PDI	Response:4 EE%
1	90	40	7.5	199.56±2.14	-13.14±1.63	0.25±0.0015	82.86±0.64
2	80	50	7.5	168.23±3.21	-19.35±1.06	0.26±0.0015	84.96±0.57
3	80	40	10	222.41±3.05	-21.26±1.89	0.23±0.0015	85.43±0.31
4	80	60	10	146.81±2.64	-19.17±1.52	0.34±0.0045	86.29±0.70
5	90	50	10	198.77±2.08	-14.54±1.41	0.41±0.007	85.81±0.58
6	90	50	5	127.61±3.05	-22.6±0.58	0.24±0.00305	83.69±1.15
7	70	40	7.5	145.28±2.08	-25.08±1.54	0.25±0.01	80.72±0.87
8	80	60	5	151.93±0.57	-21.02±1.53	0.26±0.00568	85.58±0.66
9	70	50	10	186.37±2.57	-24.2±2.67	0.23±0.00115	90.01±2.21
10	70	60	7.5	143.98±1.15	-15.3±0.752	0.34±0.001	81.58±0.57
11	70	50	5	106.12±3.98	-13.7±1.51	0.41±0.00152	82.79±0.61
12	80	40	5	97.03±2.62	-15.7±1.52	0.24±0.001	83.41±0.57
13	90	60	7.5	178.41±2.08	-25.5±0.56	0.18±0.00264	83.30±1.16

3.2. Graphical Representation of Parameters Effecting Particle Size

Table in Figure 3.1 shows that the model is significant because p value is smaller than 0.05 and the model is linear type. The difference between Adjusted and predicted R2 is 0.8576 and less than 0.2. The VIF value is within accepTable limits. The 3D graphs show the effect of several variables on particle size. Graph A and B in Figure 3.1 shows that there is direct relationship of drug and lipid concentration with the particle size. Graph A and C in Figure 3.1 also shows that by increasing the surfactant concentration there was observed reduction in the particle size while keeping other parameters constant.

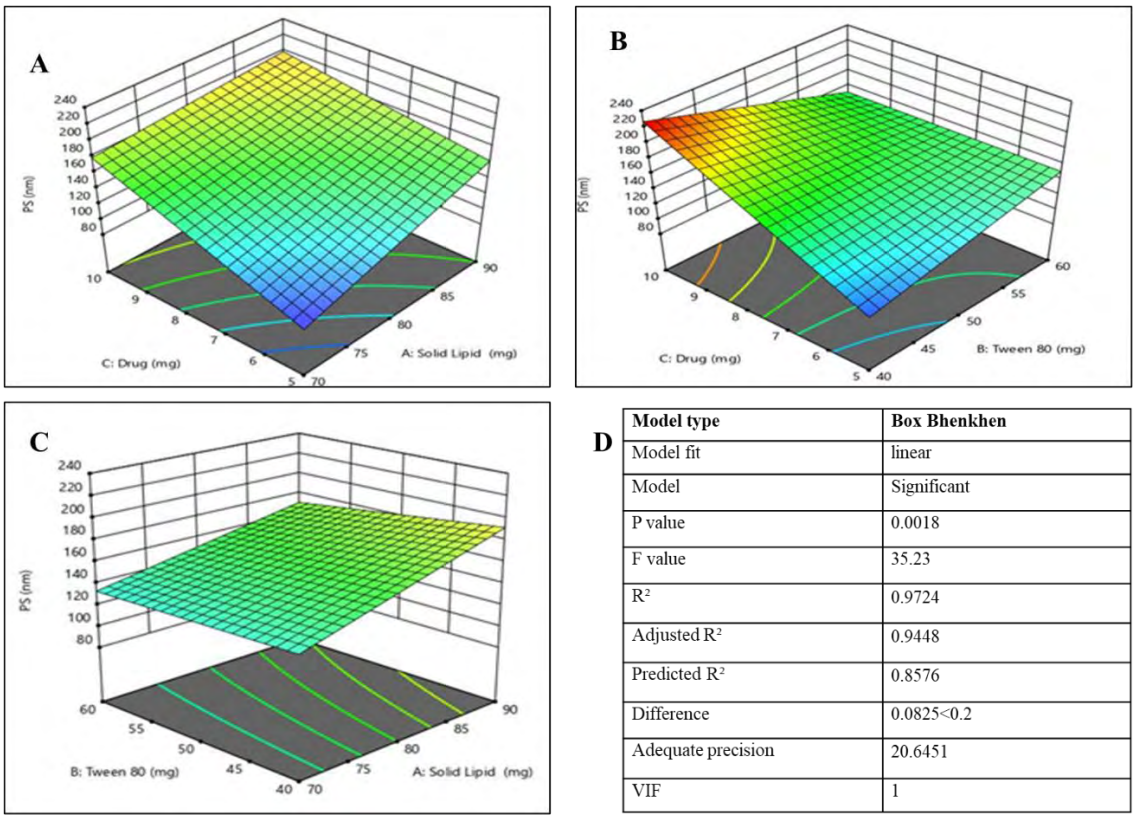

D

Model type	Box Bhenkhen
Model fit	linear
Model	Significant
P value	0.0018
F value	35.23
R^2	0.9724
Adjusted R^2	0.9448
Predicted R^2	0.8576
Difference	0.0825<0.2
Adequate precision	20.6451
VIF	1

Figure 3.1. Graphical representation of parameters effecting particle size.
***Note**: A) Effect of drug and solid lipid on PS. B) Drug and tween 80 on PS, C) Tween 80 and solid lipid on PS, D) show Table of model type linear.*

3.3. Graphical Representation of Parameters Effecting Zeta Potential

Table in Figure 3.2 shows that the model is not significant because p value is 0.0007 and the model is linear type. The difference between Adjusted and predicted R2 is 0.9419 and less than 0.2. The VIF value is also accepTable. The 3D graphs in Figure 3.2 show effect of various parameters on the zeta potential. Graph A and C in Figure 3.2 shows that there

is inverse relationship of solid lipid and drug concentration on the zeta potential while keeping the surfactant conc constant. Graph A and B in Figure 3.2 shows that there is direct relationship of surfactant on the zeta potential while keeping other parameters constant.

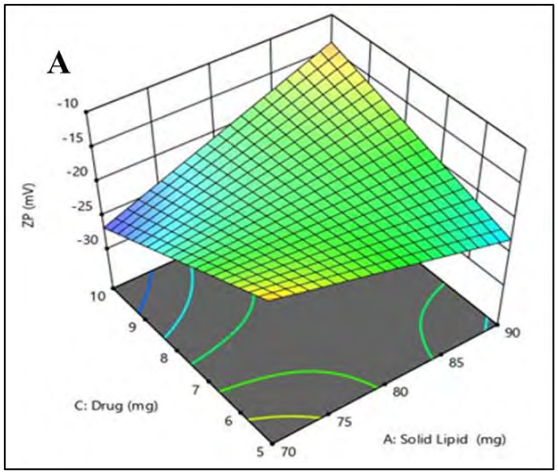

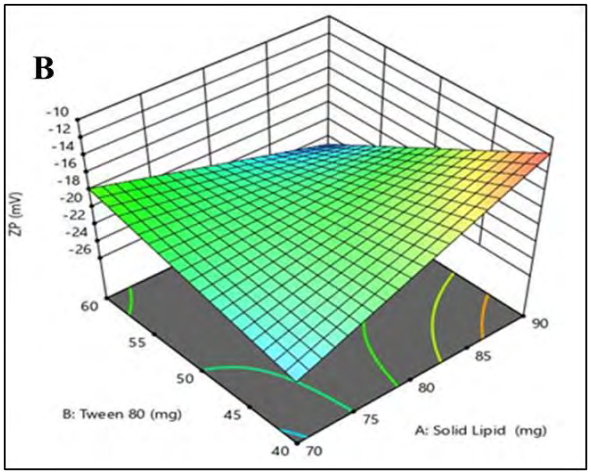

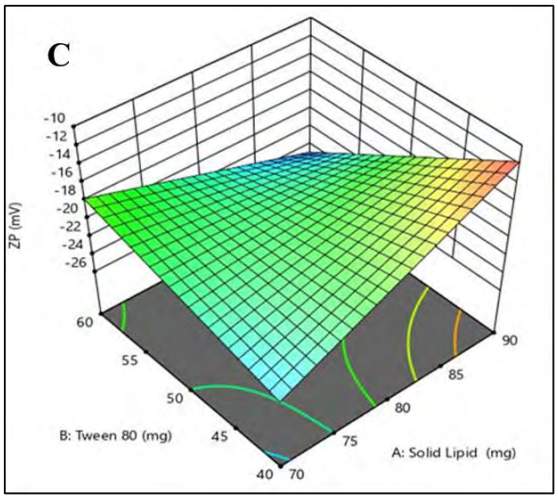

D

Model type B	**Box benkin**
Model fit	2f1
Model	significant
P value	0.0007
F value	16.22
R^2	0.9419
Adjusted R^2	0.8839
Predicted R^2	0.6844
Difference	Less than 0.2
Adequate precision	12.5926
VIF	1

Figure 3.2. Graphical representation of parameters effecting zeta potential.
***Note**: A) Effect of drug and solid lipid on ZP, B) Drug and solid lipid on ZP, C) Tween 80 and solid lipid on ZP, D) Table show model is 2fI type.*

3.4. Graphical Representation of Parameters Effecting PDI

The analyzed data for PDI shows an F-value of 5.70 and a p-value of 0.0182. The p- value indicates that the independent variables have a significant effect on the PDI. The 3-D graph shown in Figure 3.3.

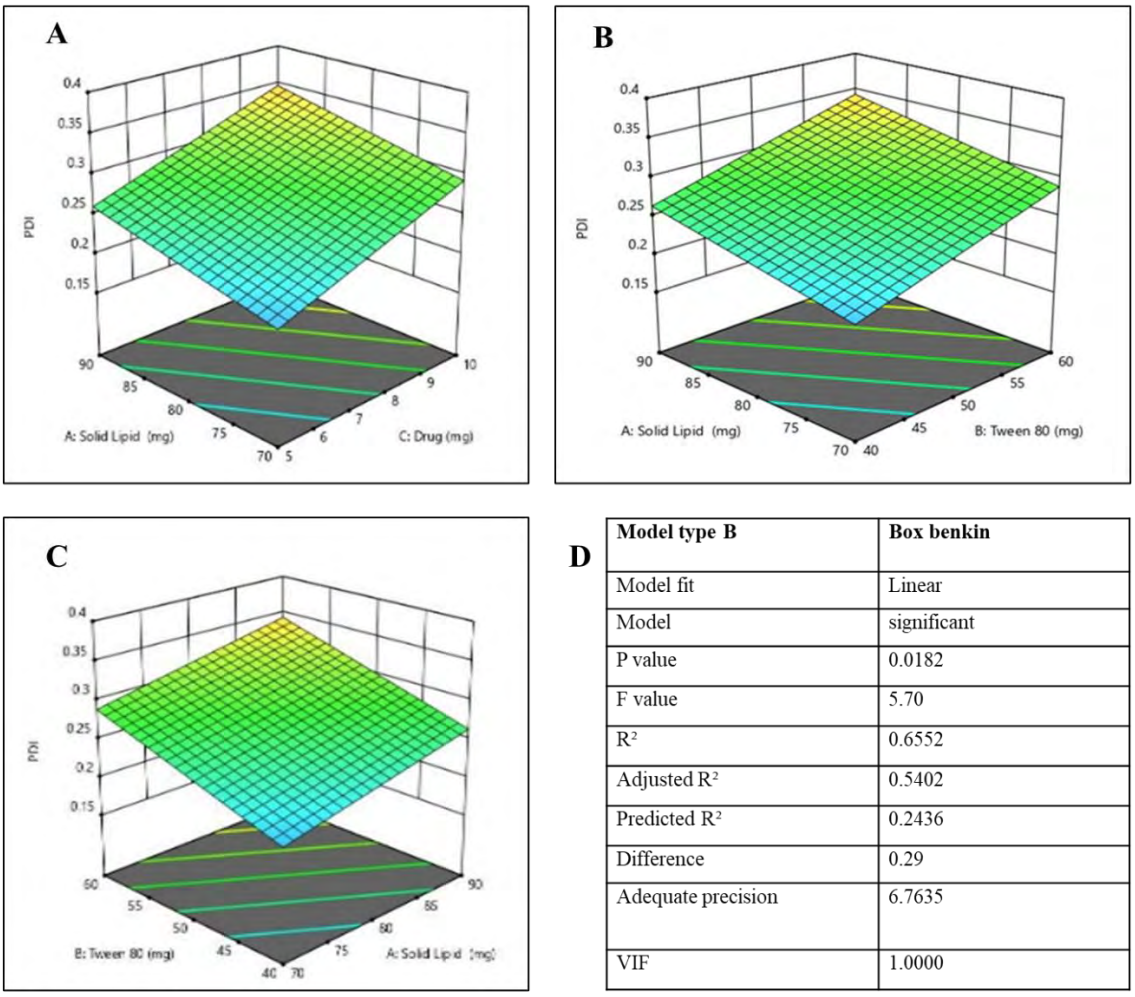

D

Model type B	Box benkin
Model fit	Linear
Model	significant
P value	0.0182
F value	5.70
R^2	0.6552
Adjusted R^2	0.5402
Predicted R^2	0.2436
Difference	0.29
Adequate precision	6.7635
VIF	1.0000

Figure 3.3. Graphical representation of parameters effecting PDI.
***Note**: A) Effect of drug and solid lipid on PDI. B) solid lipid and tween 80 on PDI, C) Tween 80 and solid lipid on PDI, D) Table show model is linear type.*

3.5. Graphical Representation of Parameters Effecting Entrapment Efficiency

Table in Figure 3.4 shows that the model is significant because p value is 0.0431 and the Quadratic model is type. The difference between Adjusted and predicted R2 is 0.8685 and less than 0.2. The VIF value is also accepTable. The 3D graphs show effect of various parameters on entrapment efficiencies of both drugs. Graph A in Figure 3.4 shows that there is direct relationship of solid lipid and surfactant on the entrapment of drugs while keeping other parameters constant. Graph B and C in Figure 3.4 shows that by increasing the drug concentration beyond certain limit may reduce the entrapment while keeping other variables constant.

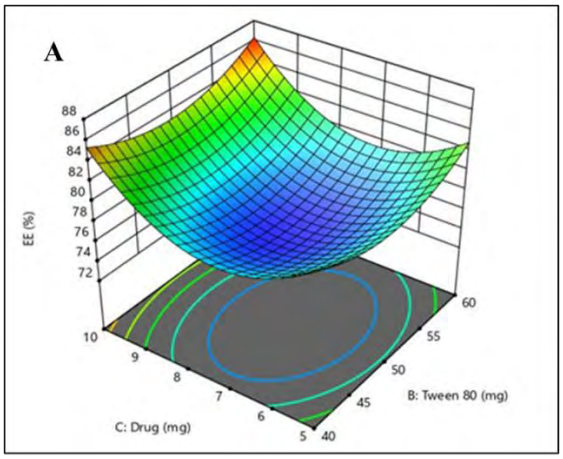

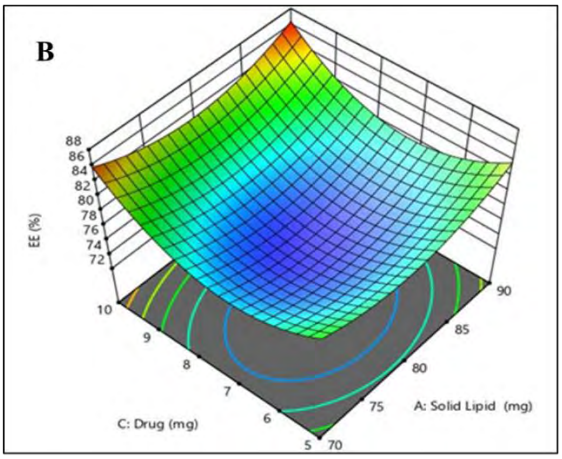

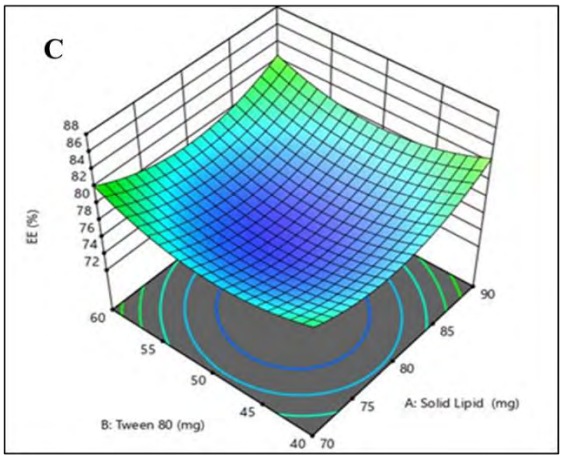

D

Model type B	Bhenkhen
Model fit	Quadratic
Model	Significant
P value	0.0431
F value	9.81
R^2	0.9671
Adjusted R^2	0.8686
Predicted R^2	
Difference	Less than 0.2
Adequate precision	11.4819
VIF	1

Figure 3.4. Graphical representation of parameters effecting entrapment efficiency.
***Note**: A) Effect of drug and Tween 80 on EE, B) Drug and solid lipid on EE, C) Tween 80 and solid lipid on EE, D) Table show model is Quadratic type.*

3.6. Characterization of MRT-Loaded NLCs

3.6.1. Particle size and PDI of optimized MRT-loaded NLCs

To determine particle size and PDI ,optimized formulation was diluted with Distlled water. Dilution with distlled water was performed ten times to measure light scattering intensity within the instrument sensitivity range.The average size of NLCs loaded MRT was 186.3 nm and PDI value was 0.217 as shown in Figure 3.5.

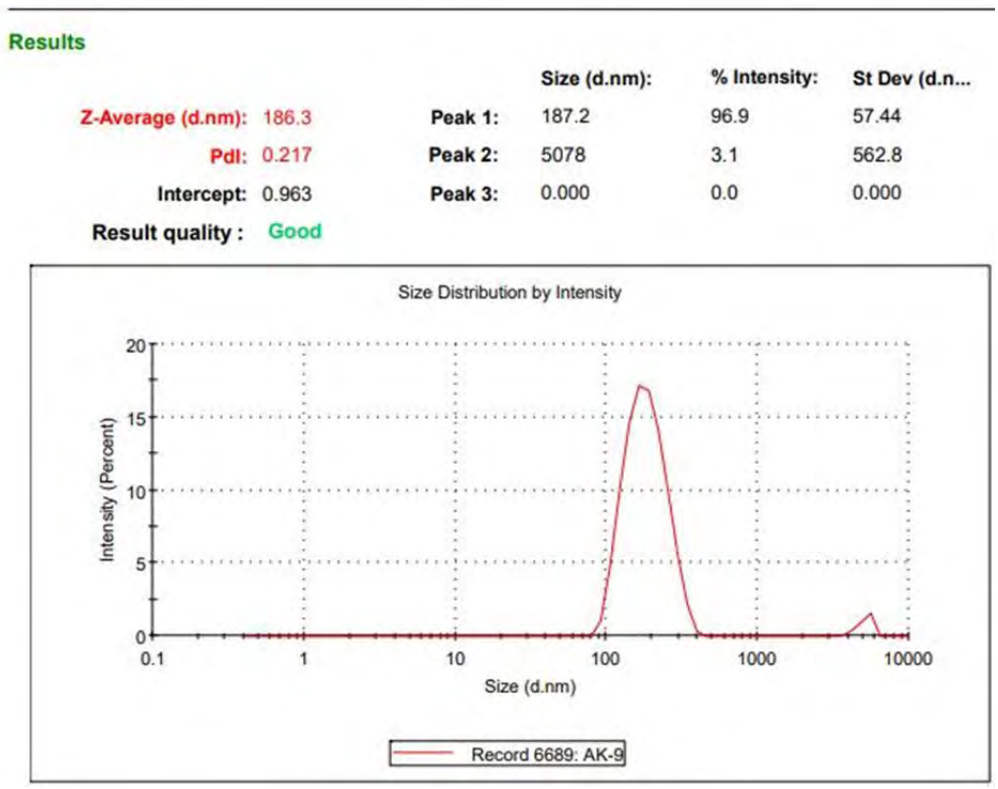

Figure 3.5. Results of particle size and PDI of optimized MRT-loaded NLCs.

3.6.2. Zeta potential of MRT loaded NLCs

It is critical parametr to detemining the stabililty of formulation.it was measured using DLS and found to be -26 mev for optimaztion formulation. It was shown in Figure 3.6 that formulation was relatively sTable.

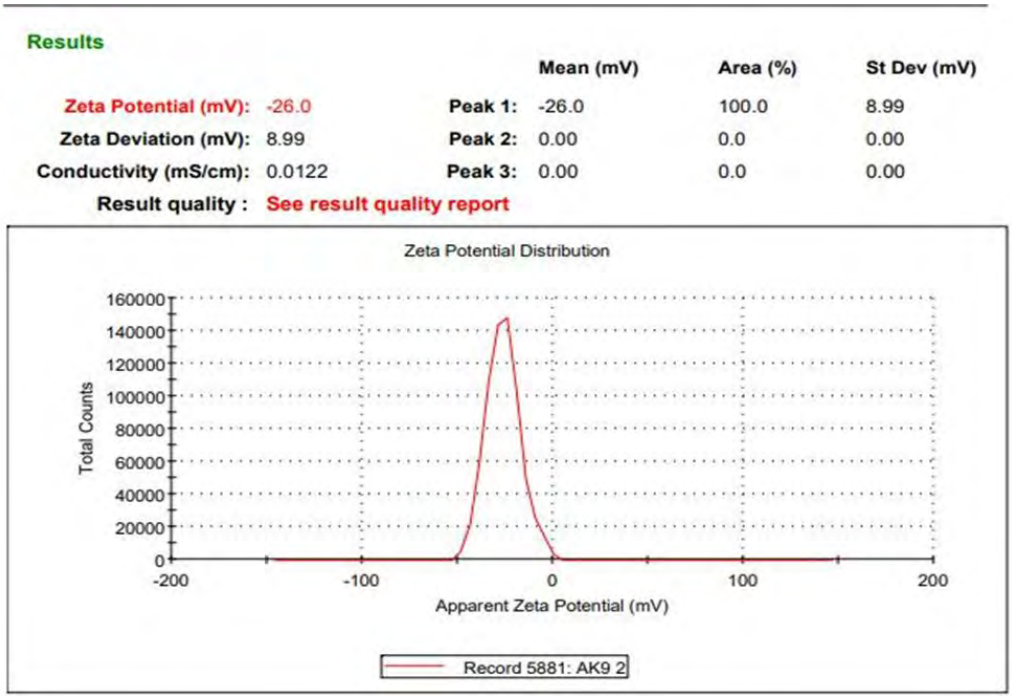

Figure 3.6. Results of zeta potential of MRT loaded NLCs.

3.7. Standard Curve of MRT In Methanol

Standard curve was generated using different concentration agaisnt the absorbance.Table.3.2 showing absorbance of different concentration using the Table we gerate a standand curve. The standard curve was used to calculate the absorbance of unknown concentration. Table 3.2 was showing the value of absorbance of different concentraion of MRT and its standard curve was shown in Figure 3.7.

Table 3.2. Absorbance of different concentration.

Serial No	Concentration µg/ml	Absorbance
1	25	0.253
2	20	0.211
3	15	0.161
4	10	0.112
5	5	0.062

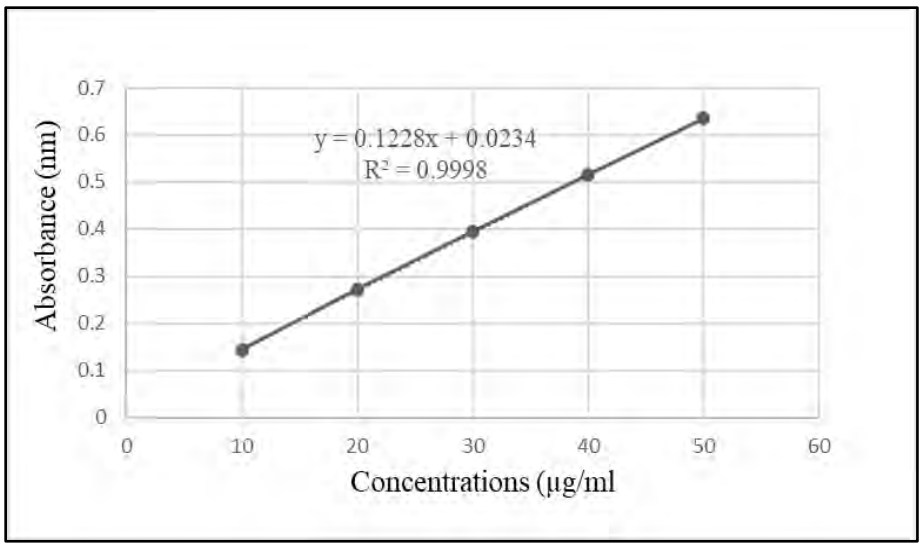

Figure 3.7. Standard Curve of MRT In Methanol.

3.7.1. Calibration curve at pH.5.5 of mirtazapine

A calibration curve was generating at pH 5.5 of mirtazapine by using different concentration and absorbance values given in Table 3.3.

Table 3.3. Different absorbance at different concentration at pH 5.5.

Serial No	Concentration µg/ml	Absorption
1	50	1.17
2	40	0.932
3	30	0.710
4	20	0.498
5	10	0.261

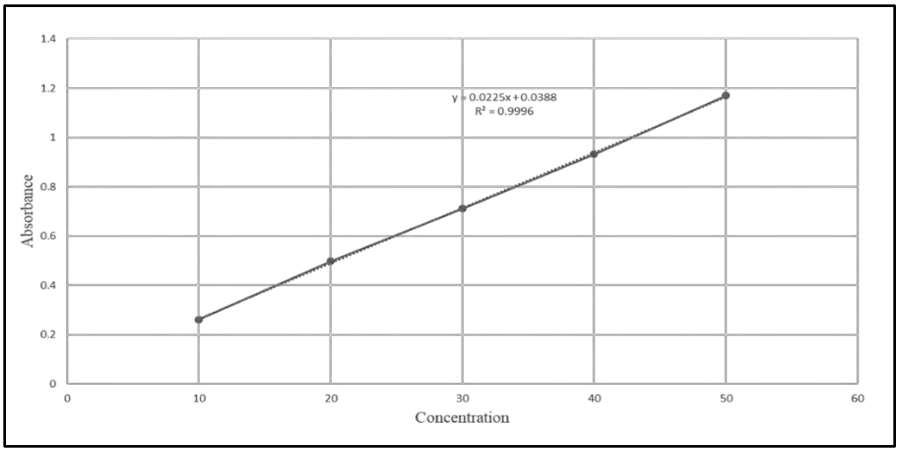

Figure 3.8. Calibration curve at pH.5.5 of mirtazapine.

3.7.2. Calibration curve at pH.7.4 of mirtazapine

Different concentration values give different absorbance as shown in Table 3.4, and these values was used to generate the calibration curve of mirtazapine at pH7.4.

Table 3.4. Values of absorbance at different concentration.

Serial No.	Concentration µg/ml	Absorbance
1	50	1.15
2	40	0.932
3	30	0.701
4	20	0.468
5	10	0.230

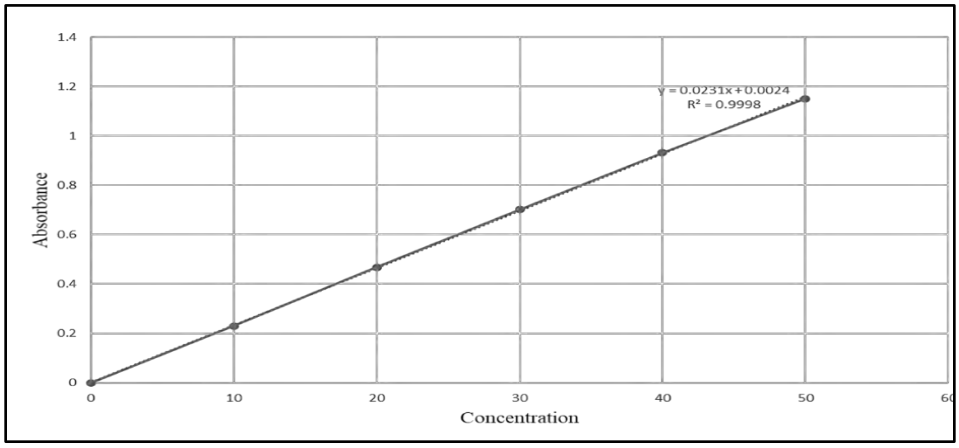

Figure 3.9. Standard curve at pH7.4 of MRT.

3.8. Entrapment Efficiency (EE)

To determine the encapsulation efficiency of MRT loaded NLCs, experiments were carried out in triplicate and average entapment efficiency of sample was 87.79 % as shown in Table 3.5.

Table 3.5. Entrapment Efficiency of different sample.

Sample	Average Absorption	Entrapment efficeincy(%)	Average EE(%)
E1	0.270	90.2	87.79
E2	0.287	87.21	
E3	0.255	85.96	

3.9. Fourier Transform Infrared Spectroscopy (FTIR)

The drug's interaction with the excipients employed in the formulation of the MRT-loaded NLCs was studied using FTIR. Characteristic peaks for MRT, Compitrol, and

physicochemical Mixture were observed in the FTIR analysis. The lyophilized MRT-loaded NLCs contained all of the peaks, ensuring that there was no drug-lipid interaction in the formulation as shown in Figure 3.10.

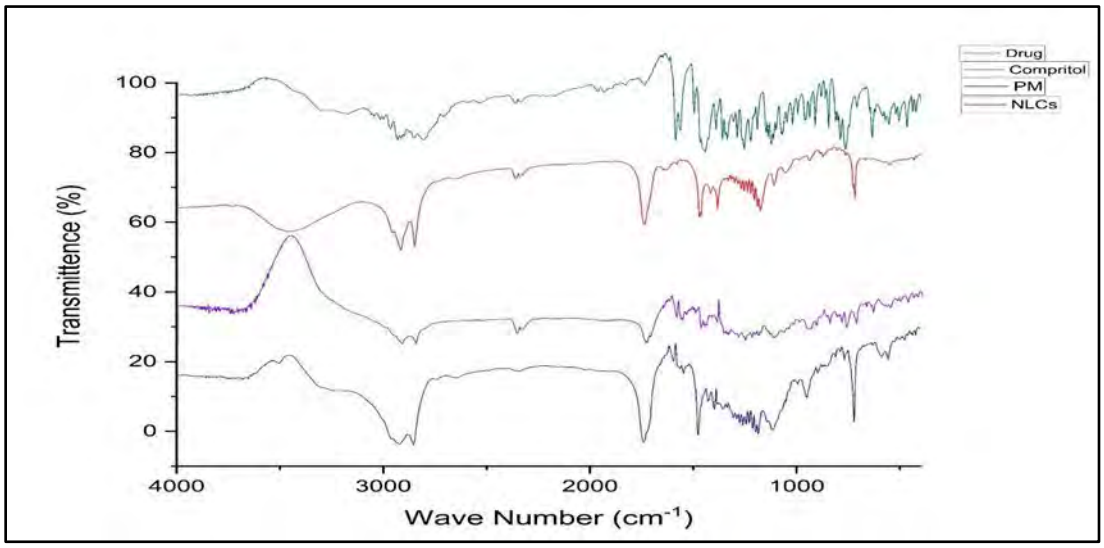

Figure 3.10. Fourier transform infrared spectroscopy of MRT.

3.10. XRD Analysis

From XRD study it was observed that pure MRT displayed high crystalline nature with characteristics diffraction peaks at 2θ of °,21°, 23° and 24° and Compitrol showed principal peak at 24° and physical Mixture also show chracterstic peaks at21°, 23° . Whenever Drug and compitrol was loaded in to the NLCs the characteristic peaks were disappeared showing the proper encapsulation and transformation of crystalline nature to amorphous form as shown in Figure 3.11.

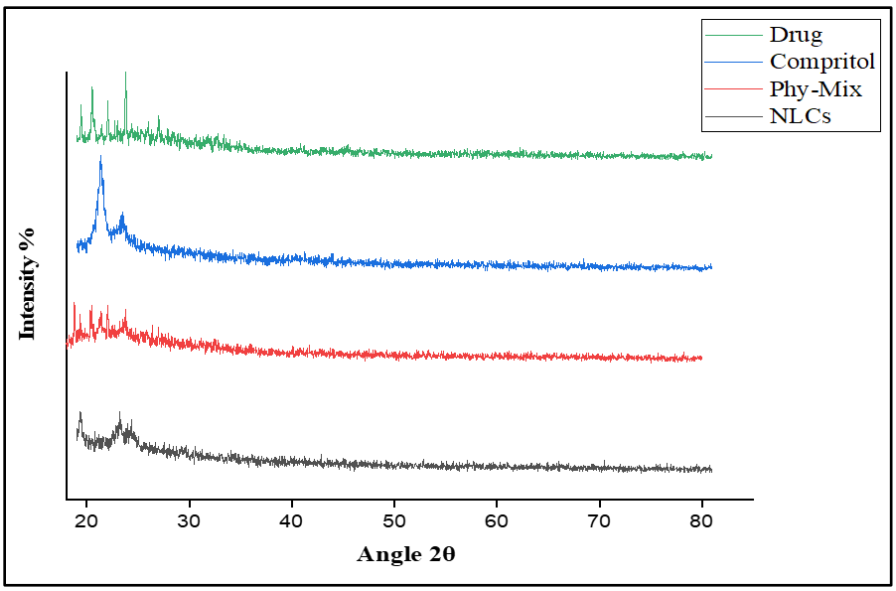

Figure 3.11. XRD Analysis of MRT.

3.11. DSC Analysis

DSC thermograms of pure MRT and lyophilized MRT-loaded NLCs showed in Figure 3.12. The melting point of MRT was disclosed by a pronounced endothermic peak at 120°C. Pure MRT displayed a substantial endothermic event at 120 °C, which corresponded to its melting point, demonstrating the crystalline structure of the pure drug. The peak for drugs was reduced in lyophilized MRT-loaded NLCs showed amorphous structure as shown in Figure 3.12

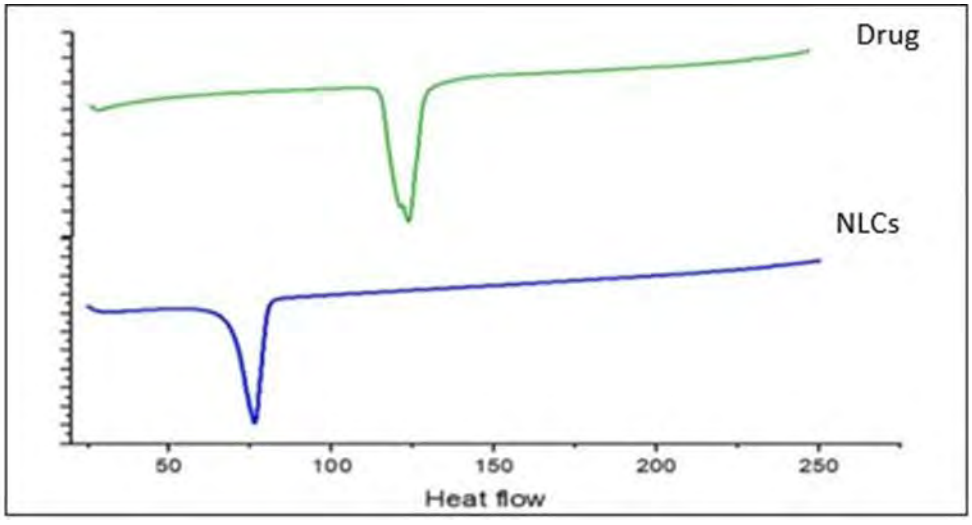

Figure 3.12. DSC analysis of MRT.

3.12. Preparation of MRT-Loaded NLCs Gel

The gel was prepared successfully from Chitosan low molecular weight, glutaraldehyde, and Triethylamine. The final gel was 2% of Chitosan shown in Figure 3.13.

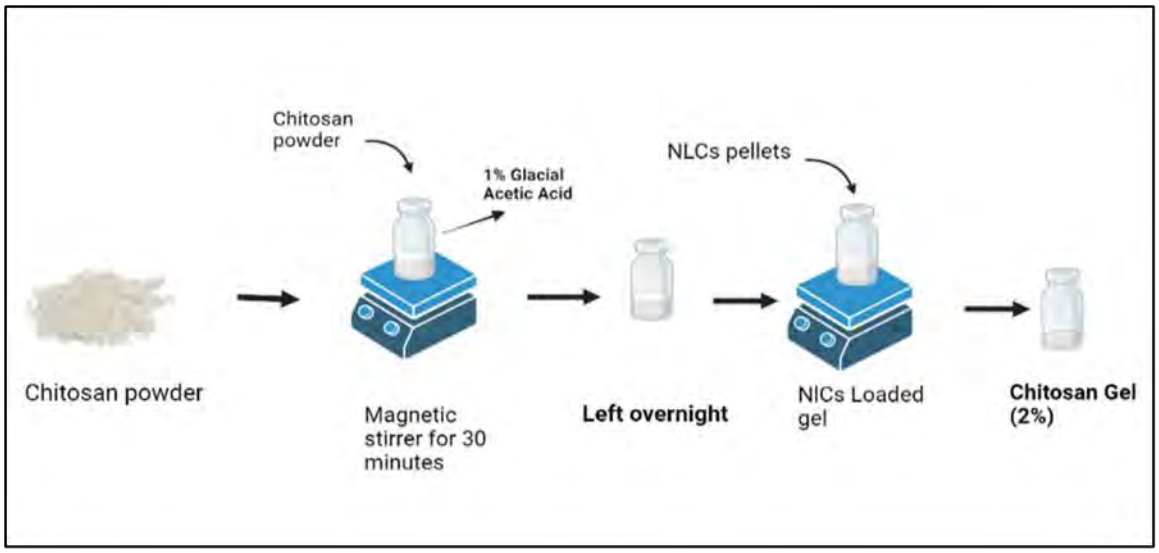

Figure 3.13. Pictorial presentation of preparation of MRT NLCs loaded gel.

3.13. MRT-loaded NLCs Gel Characterization

3.13.1. Homogeneity and visual appearance

The prepared MRT-loaded NLCs gel appeared Clerance and opaque. The gel was free of any gritty particles or clumps, indicating its homogeneity.

3.13.2. Drug content

The average drug content in 2% chitosan gel was calculated to be 98.27% as shown in Table 3.6.

Table 3.6. Drug content of MRT NLCs.

Serial No	Drug content(%)	AVG+STD(%)
1	98.6	98.27±0.2858
2	98.1	
3	98.11	

3.13.3. Spreadability of MRT-loaded NLCs gel

The mean spreadability of formulation loaded gel was indicating good Spreading characteristics. Tabie 3.7 was showing 322.33± 0.25% spreadability value of MRT-loaded NLCs gel.

Table 3.7. Spreadability of MRT-loaded NLCs gel.

Serial No	Abservation	AVG+STD
1	325%	322.33± 0.25%
2	320%	
3	322%	

3.13.4. pH of MRT-loaded NLCs gel

The pH of MRT-loaded NLCs gel was determined and it was 5.9±2.02 as shown in Table 3.8, which considered suiTable for dermal application.

Table 3.8. pH of MRT-loaded NLCs gel.

Serial No	pH	Average pH
1	5.7	5.9±2.02
2	5.9	
3	6.2	

3.13.5. Rheological study

By increasing the shear rate, the viscosity of the chitosan gel decreased from 8412 to 1565 cP. It showed non- newtonian flow as shown in Figure 3.14.

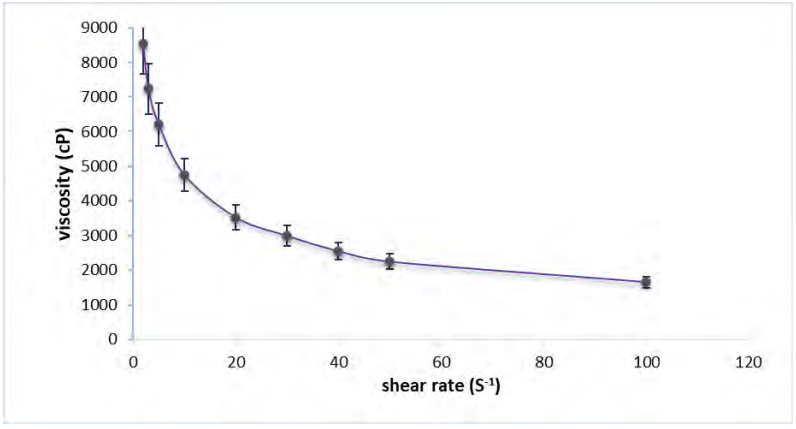

Figure 3.14. Rheology study of MRT Gel.

3.13.6. *In vitro* drug release at pH 5.5

The cumulative percentage drug release from the optimised NLCs dispersion, NLCs gel, MRT(drug) dispersion, and MRT loaded gel over the period of 24 hours at pH 5.5 was assessed. The in vitro drug release profile curves and results are displayed in Figure 3.15 A biphasic pattern of drug release was seen in both the NLCs gel and the NLCs dispersion, with an initial burst release followed by a sustained release.in case of dispersion of pure drug and pure loaded drug was obsorved that 100% drug release within 4-6 hours.NLCs dispersion showed 44% release in first hour show brust release then follow sustain release upto 92% in 24 hours and NLCs gel release 34% in first hour then follow sustain release upto 81% in 24 hours as indicated by Figure 3.15.

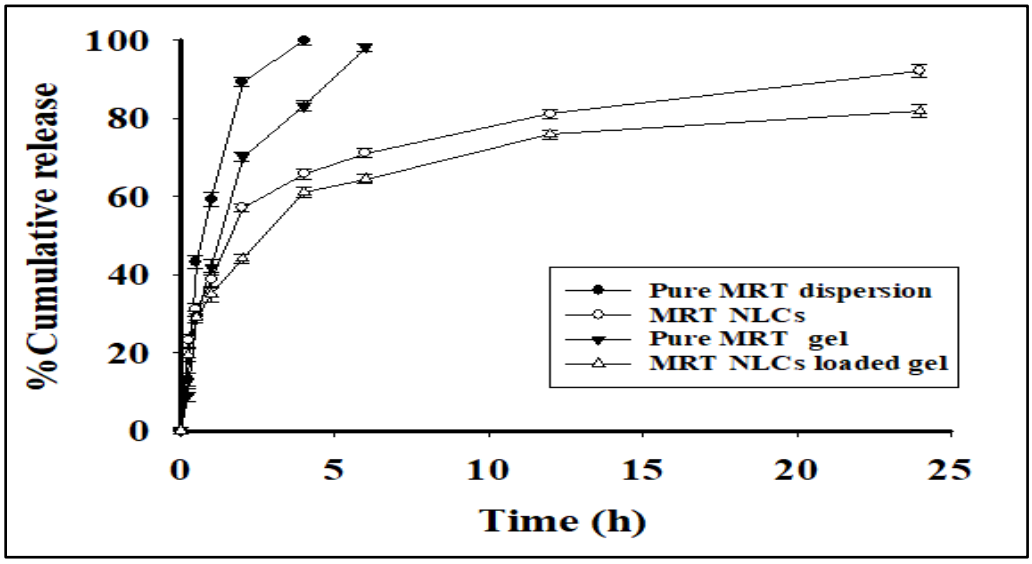

Figure 3.15. Drug release at pH 5.5

3.13.7. *In vitro* drug release at pH 7.4

The in vitro release behavior of of MRT dispersion pure drug gel and MRT-loaded NLCs and MRT-Loaded NLCs gel gel were also evaluated at pH 7.4, that is the pH of blood. MRT Dispersion and gel showed 21.11% ,17.29. in 2 hrs and 51% ,41% release within 24 hrs due to low solubilty in aqoaus phase, while MRT-NLCs loaded,MRT loaded gel has given 43.11%,33.1% release in first 2 hrs and 77.1% ,63.2% of the drug librated in 24 hrs as shown in Figure 3.16.

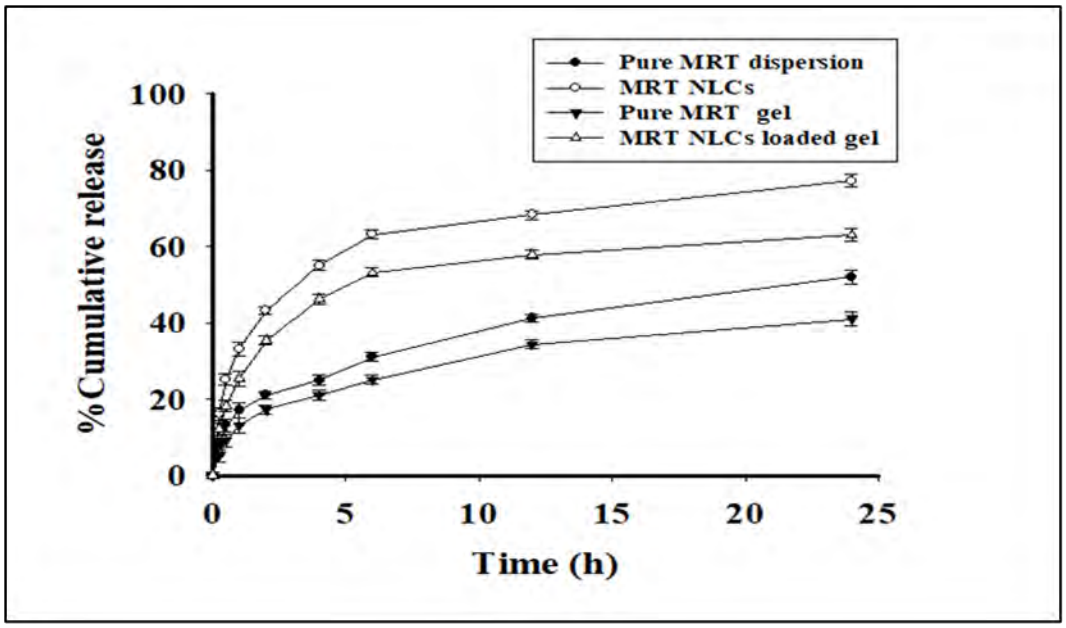

Figure 3.16. Drug release at pH 7.4.

3.14. *Ex Vivo* Releases Study

The ex vivo release behavior of MRT-loaded NLCs gel and pure drug gel was carried out through fraz diffusion cells. The conc of drugs released was plotted against time (hr). The nanoparticle loaded gel showed greater permeation than pure loaded gel. At 24 hr NLCs gel and Pure gel permeated 6.4mcg/cm² and 2.4 mcg/cm² as shown in Figure 3.17.

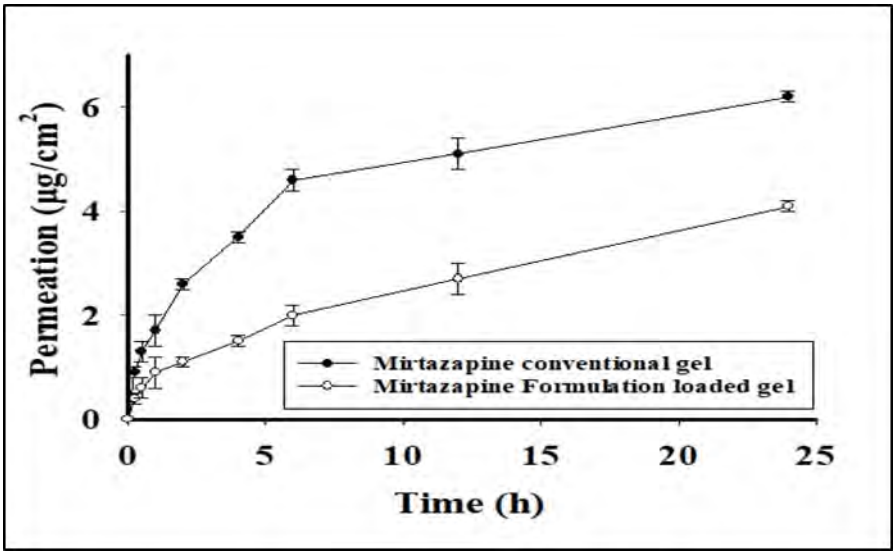

Figure 3.17. *Ex vivo* release study of MRT Gel.

3.15. Drug Release Kinetics

Zero order, first order, higuchi model and korseymeres-papas model were applied to determine the best fit model based on R^2 and n values.

3.16. Kinetic Release Model Table

In order to suggest the feasible release pattern from NLCs dispersion and NLCs gel, the release data was analyzed to check the goodness of fit into different kinetic models namely zero order, first order, Higuchi, Hixon-Crowell and Korsmeyer Peppas models. The model with the highest value of correlation coefficient (R2 was chosen as best model to describe the release kinetic of drug from the formulations. In case of NLCs dispersion, the R2 values obtained by fitting the release data into different models indicate that the best fit model is Highuchi model having highest R2 value (i.e., 0.9895) as shown in Table 3.9.

Table 3.9. Kinetic release parameters.

formulation	Zero order		First order		Higuchi		Hixon crowel		Korsmeyer-peppas	
	R2	Ko	R2	K1	R2	Kh	R2	Khc	R2	Kkp
NLCs	0.8420	5.208	0.9248	0.340	0.9851 n=0.857	2.392	0.9434	23.938	0.9748	0.060
NLCs gel	0.8386	4.696	0.9788	0.024	0.9895 n=0.273	37.010	0.9438	21.548	0.9819	0.053

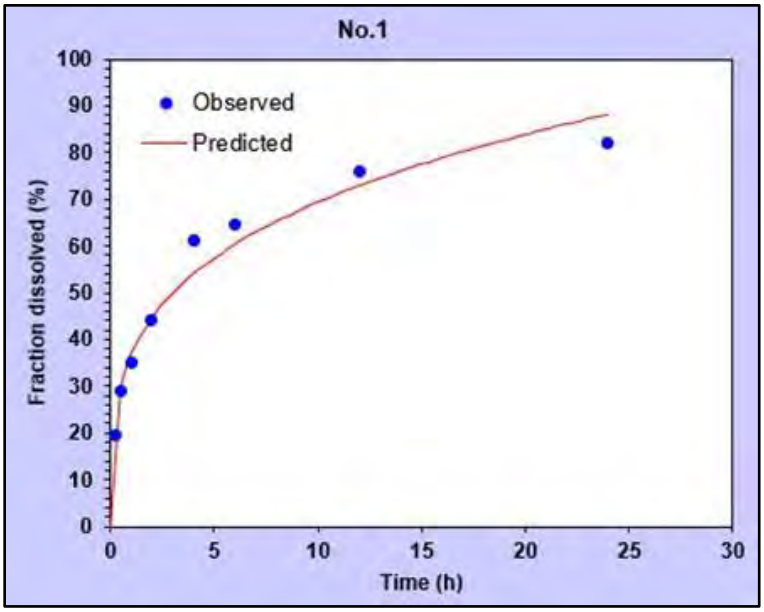

Figure 3.18. MRT Predicted observation.

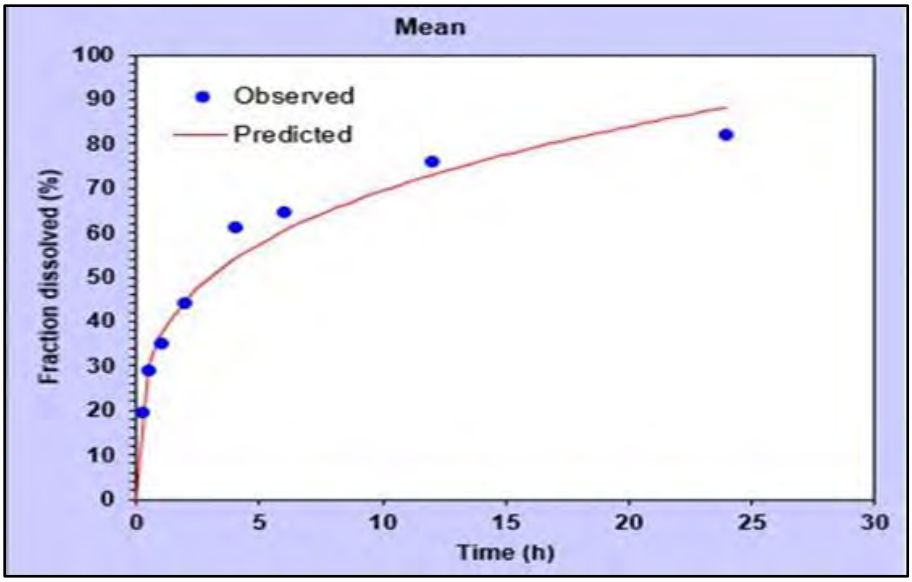

Figure 3.19. MRT Predicted observation Mean.

3.17. Stability Study

Table 3.10 and Table 3.11 showing the real time stability testing at 4 degree and 5 degree respectively.

Table 3.10. Real time stability testing at 4°C.

Time in months	Physical appearance			Drug content	pH
	Color change	Grittiness	Phase separation		
After 1 month	No	No	No	98.49±1.29	5.81±0.02
After 2 months	No	No	No	97.71±1.31	5.94 ± 0.028
After 3 months	No	No	No	97.12±1.55	6.21 ± 0.02

Table 3.11. Stability study at room temperature 25°C.

Time in months	Physical appearance			Drug content	pH
	Color change	Grittiness	Phase separation		
After 1 month	No	No	No	98.11±1.29	5.98±0.11
After 2 months	No	No	No	97.71±1.31	6.09±0.09
After 3 months	No	No	No	97.12±1.55	6.71±0.29

3.18. Skin Irritation Study

The skin irritation was evaluated using the Draize grading system. When compared to the PDII of 3.66 in the traditional formalin treated group, the PDDI MRT-loaded NLCs of 0.11 are not statistically significant. The results from the examination into skin irritation are displayed in Figure and Tables 3.12 and 3.13. Histopathological findings supported the in-vivo skin irritation investigation's conclusion. The skin tissue damage in the formalin-treated group was evident from the skin irritation research's histological findings, which are shown in Fig 3.20. Skin tissue damage was not present in the group treated with the MRT-loaded NLCs gel. The scoring criteria for edma and erythematous skin are given in Table 3.12 and 3.13. The histopathological changes was shown in Figure 3.20

Table 3.12. Scoring criteria for edema.

Assessment of skin edema score	12 hours	24 hours
Normal control	0	0
Negative control	1	2
Gel treated	0	0
Total	01	02

Table 3.13. Scoring criteria for erythematous skin.

Assessment of skin erythema score	12 hours	24 hours
Normal control	0	0
Negative control	2	3
Gel treated	0	0
Total	02	03

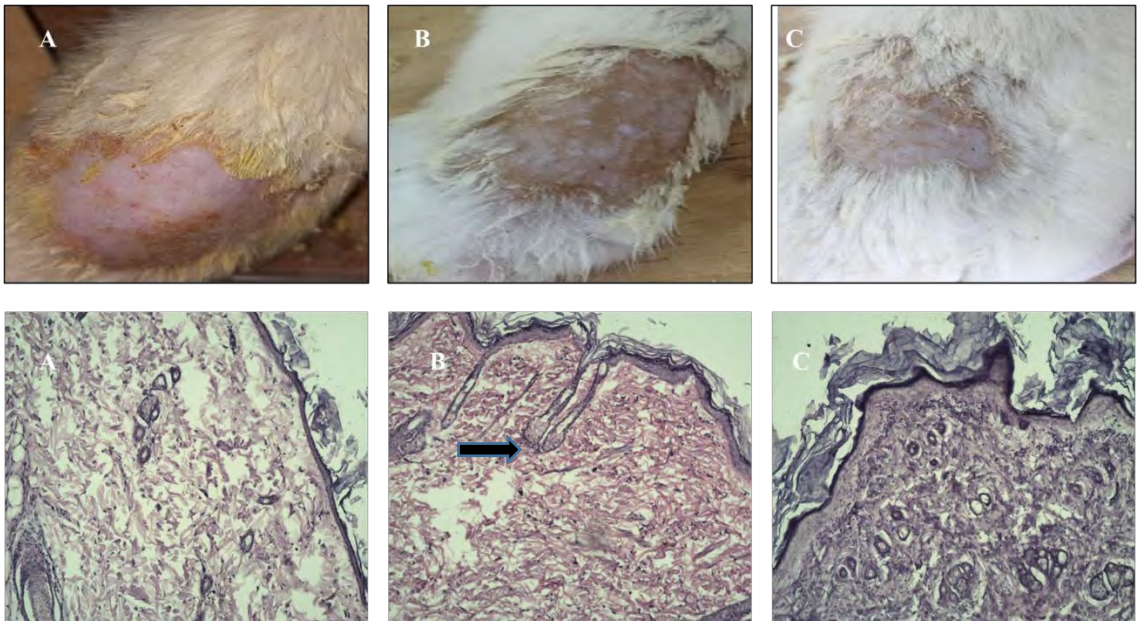

Figure 3.20. Effect of MRT gel on Histopathology of irritated skin at 10X.
NOTE: *A: Showing normal skin, B: Formalin treated skin, C: Gel treated skin. Black arrow is showing the inflammation in formalin treated group in B. Whereas in A and C there is no inflammation.*

CHAPTER 4

DISCUSSION

4. DISCUSSION

The aim of current study to develop the lipid base nanocarrier system with MRT for the treatment of pruritus by incorporating MRT loaded NLCs in the chitosan gel for topical applications. The study's main theme was to overcome the shortcomings of commercially available products and to enhance the treatment effect of the prepared formulation.. (Sharma *et al.*, 2020). A biodegradable lipids Compitrol and oleic acid which has permeation enhancing properties were selected for the preparation of NLCs. Due to the biocompatibility and flexibility of lipids, lipid-based nanoparticles have been found to offer a potential in the treatment of skin disease. Due to improved drug stability, improved skin permeability, retention, and therapeutic efficiency, nanostructured lipid carriers (NLCs) have drawn a significant amount of attention in the treatment of skin diseases. The study reviews the NLCs' properties and their use for topically delivering different treatments for skin disorders NLCs have demonstrated significant promise in the efficient delivery of drugs for the treatment of psoriasis, dermatitis (pruritus) (Waghule *et al.*, 2020).

Surfactants (such as Tween 80) can also be used to prevent particle aggregation. It was fo und that a surfactant blend can effectively stop (Mehnert and Mäder, 2012). The modified micro-emulsion method was used to prepare MRT-loaded NLCs. This method was selected over others because of its easiness, affluence of production, lower energy requirements, and ability to be carried out using the most basic laboratory equipment available (Suksaeree *et al.*, 2020).

for the optimization of formulation MRT loaded NLCs Using Design Expert version 12 the Box Behnken model. Thirteen formulations were developed by altering the lipids, drug, and surfactant concentrations. These modifications' effects on particle size, entrapment effectiveness, and zeta potential were displayed in Table 3.1. The software's evaluation of all the runs based on predetermined goals for size polydispersity index, entrapment efficiency, and zeta potential led to the selection of the optimised formulation. PDI of 0.230.0011, zeta potential of -24.22.67, entrapment of 86.612.21 and particle size of 186.372.57 nm are all characteristics of an optimised formulation.

Increase in concentration of solid lipid from 70 to 90 mg (7:3-9:1) leads to increase in particle size. It shows Linear model shown in Figure 3.1. Similarly, with increase in

concentration of surfactant from 40 to 60 mg, particle size decreases slightly and then becomes constant and at the end increases slightly so a non-significant effect was observed in this case. According to the literature, increasing solid lipid increases particle size whereas increasing surfactant decreases particle size. The reason for this is that as the solid lipid concentration increases, the liquid lipid concentration falls, resulting in an increase in viscosity and interfacial tension, which leads to increased particle size. Similarly, increasing surfactant concentration reduces particle size by lowering surface tension and interfacial tension between particles, resulting in smaller particle size (Yoon *et al.*, 2013). Decreased solid lipid concentration means more liquid lipid concentration that reduces viscosity and in turn reduces interfacial tension so particle size, almost same results were reported by (Sanad *et al.*, 2010).

The particle size increased significantly. Similarly, to this, a non-significant increase in particle size was observed at lower drug concentrations after a decrease. Increased viscosity of molten lipid causes difficulty in two phase dispersion, which causes particle size to increase due to higher drug content, as was observed in the literature in the instance of oxybenzone NLCS (Sanad *et al.*, 2010). Effect of drug and surfactant on particle size also shows a Linear model with similar results as in previous case. Result was shown Figure 3.1.

There was no significant effect observed on PDI with changes in concentrations of solid lipid, surfactant, and drug. Linear model was observed in this case shown in Figure 3.3.

In case of zeta potential, the suggested model was 2f1. Increase in solid lipid concentration changes zeta potential from -24.9 mV to -17.6 mV. Changes concentration of surfactant from 40 to 60 mg, zeta potential becomes more negative. The zeta potential value indicated the stability of nanoparticles. Nanoparticles with a zeta potential larger than ± 25 mV are said to be sTable at highest concentration of solid lipid, zeta potential was less and then with decrease in solid lipid concentration, zeta potential increases while drug concentration remained constant. Because of the reduction in particle size, which could increase the charge density on the surface of nanoparticles, a drop in solid lipid concentration leads to an increase in zeta potential value. The effect of solid lipid and surfactant concentration on the zeta potential value is shown in Figure 3.2 A At high drug concentration, zeta potential

was high and with increase in concentration, zeta potential becomes more. Reduced solid lipid concentration increases zeta potential as particle decreases that leads to high charge density on the nanoparticles (Han *et al.*, 2012).the result shown in Figure 3.2.

Figure 3.4 depicts the effect of solid lipid and Drug concentrations on % EE when the surfactant concentration is held constant. Increase in surfactant concentration leads to a slight decrease in entrapment efficiency and increase in concentration of solid lipid, results in a significant rise in entrapment efficiency. In this case, quadratic model was observed. Increasing solid lipid increases entrapment efficiency. At lower drug concentration, entrapment efficiency was low and by increasing drug concentration, entrapment was increased but in a non-significant way. Increasing surfactant concentration decreases entrapment in a non-significant manner. The influence solid lipid and drug concentrations on percent EE is shown when surfactant concentration is held constant. When the concentration of solid lipid was increased, the % EE increase. The decrease in solid lipid concentration eventually leads to an increase in liquid lipid concentration, increasing drug solubility in the NLC matrix and potentially causing crystal order disruption, which results in many defects in the NLC matrix and a decrease in% EE. The findings concurred with Sanad's (Sanad RA et al., 2010). Because the amount of lipid available to accept escalating drug concentrations may be insufficient, a decrease in % EE was seen as drug concentration was increased above a certain limit (Maqsood *et al.*, 2022).

The interaction between the drug and excipients was evaluated using FTIR. In to confirm that there was no chemical change detected because of formulation development, the presence of major bonds was observed in the physical mixture as well as in the resulting formulation using the spectrum of MRT, compritol 888 ATO®, oleic acid, and MRT-NLCs. Peaks of CH alkane were seen at 2800–3000 cm1, and vibrations at 3368.85 and 3104.78 cm revealed NH of aromatic, amide, CH of the functional group’s methyl and methylene at 2964.91 band 2812.64 cm 1. The amide group's C=O stretching was at 1615.68 cm. C-C aromatic groups are at 1615.68 cm^{11}. C-C aromatic groups at 1544.49 cm. The shifting of characteristic peaks indicates that drug succeeded to incorporate in the lipid core (Kaur *et al.*, 2018).

Physical and chemical characteristics including solubility, melting point, release pattern, and encapsulation efficiency can be affected by the drug's polymorphic forms as well as by lipids and excipients. The crystallinity of the formulation is determined by XRD. To determine the formulation's crytallinity, XRD analysis of compritol 888 ATO, MRT, physical mixture, and MRT-NLCs was performed. In order to confirm the amorphous form and drug loading, Compritol 888 ATO® had classic crystalline peaks, MRT displayed peaks at 19 angles between 19 and 30", and MRT-NLCS did not exhibit any peak (Kaur *et al.*, 2018)

DSC was used to analyse the formulation's characteristics and thermal behaviour. DSC was used to analyze the drug and lipid polymorphism states to find out how the drug and lipid interacted and how crystallinity changed. Compritol 888 ATO, MRT, and physical combination all showed distinct endothermic peaks, and MRT-NLCS displayed a modest expanded peak that denotes decreased crystallinity. This narrow peak is caused by the binary lipid core melting, which also caused the crystallinity to decrease (Kaur *et al.*, 2020).

The prepared gel was homogenously dispersed without lumps formation. The prepared gel has slightly opaque color due to the addition of MRT. The drug content was indicating consistent dispersion of the drugs (Jagdale and Pawar, 2017).The MRT -loaded NLCs gel has 6.9 pH, as it is previously reported that both acidic and basic pH may cause skin irritation (Kaur *et al.*, 2015). MRT-loaded NLCs gel has spreadability index of 322, showing desirable spreadability for topical formulation (Khaleeq *et al.*, 2020). As a rule, that more spreadability incurs feasibility to administer (Rabia *et al.*, 2020).

The variables evaluated for mirtazapine loaded NLCs gel storage at ambient and refrigerated temperatures were tabulated. The physical characteristics of con gel slightly changed after three months of storage at ambient temperature, but they remained consistent when kept in the refrigerator. The gel's TDC was discovered to be somewhat decreased at both temperatures after three months. Also, it was discovered that the formulation's viscosity decreased with time under both storage conditions (Kaur *et al.*, 2020).

Skin irritation was determined using the Draize score system., as shown in the Table. 3.12,3.13. The PDI was calculated based on the presence of erythema and edoema. A score of zero indicates no edoema or erythema, a score of one indicates very slight, a score of

two indicates slight, a score of three indicates moderate, and a score of four indicates severe erythema and edoema. The average erythema and oedema at that specific interval were used to calculate the PDI value. PDII was calculated by dividing the PDI score at each interval by the number of intervals.

CONCLUSIONS

- The Box benkin design was used to successfully developed, characterize, and optimize MRT-loaded NLCs for topical administration. The effect of different variables includes solid lipid drug concentration and surfactants on NLC particle size, Zeta potential PDI, and %EE was studied.
- The developed NLCs were found to possess advantageous physicochemical characteristics for topical drug delivery.
- Furthermore, the NLCs were incorporated into a gel having pseudoplastic flow behavior and an excellent texture for topical administration. In vitro study, the produced NLCs and gel demonstrated a biphasic release pattern, with an initial burst release. followed by sustain release.
- Ex vivo drug permeation experiments demonstrated that the produced NLCs gels more permeate than pure gel in terms of skin penetration efficiency.
- Skin irritation proved the gel's potential for topical administration and demonstrated the skin safety of the produced NLCs.
- The term "Stability" refers to the ability of a product to withstand extreme temperatures. The gel of mirtazapine loaded NLCs may be a promising formulation for the topical treatment of pruritus as a result of the above findings.

FUTURE PROSPECTIVES

- Determine the efficacy and bioavailability of MRT-loaded NLCs Dermo kinetic and In-vivo pharmacodynamic studies should be performed.
- Transdermal drug delivery of MRT-loaded NLCs for treatment of depression.

REFERENCES

REFERENCES

Ahad A, Al Saleh AA, Al Mohizea AM, Al Jenoobi FI, Raish M, Yassin AEB, Alam MAJB and Pharmacotherapy (2017). Pharmacodynamic study of eprosartan mesylate-loaded transfersomes carbopol® gel under dermaroller® on rats with methyl prednisolone acetate-induced hypertension. Biomed Pharmacother, 89: 177-184.

Alonso-Llamazares J, Rogers, Oursler JR and Calobrisi SD (1998). Bullous pemphigoid presenting as generalized pruritus: Observations in six patients. Int J Dermatol, 37 (7): 508-514.

Alves MP, Raffin RP, Fagan SBJN and Care (2011). Rheological behavior of semisolid formulations containing nanostructured systems. R dos Andradas, (11): 37-45.

Bernhard JD (2005). Itch and pruritus: What are they, and how should itches be classified. Dermatol ther, 18 (4): 288-291.

Bhaskar K, Mohan CK, Lingam M, Mohan SJ, Venkateswarlu V, Rao YM, Bhaskar K, Anbu J, Ravichandran VJDd and pharmacy i (2009). Development of sln and nlc enriched hydrogels for transdermal delivery of nitrendipine: In vitro and in vivo characteristics. Drug Dev Ind Pharm, 35 (1): 98-113.

De Boer T (1995). The effects of mirtazapine on central noradrenergic and serotonergic neurotransmission. Int Clin Psychopharmacol, 4:19-23.

Elmowafy M, Samy A, Abdelaziz AE, Shalaby K, Salama A, Raslan MA, Abdelgawad MAJB-SUjob and sciences a (2017). Polymeric nanoparticles based topical gel of poorly soluble drug: Formulation, ex-vivo and in vivo evaluation. Int J Basic Appl Sci, 6 (2): 184-191.

Han F, Yin R, Che X, Yuan J, Cui Y, Yin H and Li (2012). Nanostructured lipid carriers (nlc) based topical gel of flurbiprofen: Design, characterization and in vivo evaluation. Int J Pharm, 439 (1-2): 349-357.

Ikoma A (2009). Analysis of the mechanism for the development of allergic skin inflammation and the application for its treatment: Mechanisms and management of itch in atopic dermatitis. J Pharmacol Sci, 110: 265-269.

Jagdale S and Pawar SJ (2017). Gellified emulsion of ofloxacin for transdermal drug delivery system. Adv Pharm Bull, 7 (2): 229-230.

Jaiswal P, Gidwani B, Vyas A, nanomedicine, and biotechnology (2016). Nanostructured lipid carriers and their current application in targeted drug delivery. Nanomed Biotechnol, 44 (1): 27-40.

Karaşen N, Altinöz and analysis b (2000). Determination of mirtazapine in Tablets by uv spectrophotometric and derivative spectrophotometric methods. J Pharm Biomed Anal, 24 (1): 11-17.

Kaur L, Jain SK and Singh KJ (2015). Vitamin e tpgs based nanogel for the skin targeting of high molecular weight anti-fungal drug: Development and in vitro and in vivo assessment. . J Pharm Biomed Anal, 5 (66): 53671-53686.

Kaur R, Sharma N, Tikoo K and Sinha (2020). Development of mirtazapine loaded solid lipid nanoparticles for topical delivery: Optimization, characterization and cytotoxicity evaluation. RSC Adv, 586: 119439.

Kaur R, Sinha B (2018). Use of thermal and non thermal techniques for assessing compatibility between mirtazapine and solid lipids. Int J Pharm, 161: 144-158.

Khaleeq N, Din FU, Khan AS, Rabia S, Dar J and Khan GM (2020). Development of levosulpiride-loaded solid lipid nanoparticles and their in vitro and in vivo comparison with commercial product. J Microencapsul, 37 (2): 160-169.

Kumar N, Goindi S, Saini B, Bansal G (2014). Thermal characterization and compatibility studies of itraconazole and excipients for development of solid lipid nanoparticles. J Therm Anal Calorim, 115: 2375-2383.

Liu CH, and Wu CT (2010). Optimization of nanostructured lipid carriers for lutein delivery. Physicochem Eng Asp, 353 (2-3): 149-156.

Maqsood S, Din FU, Khan SU, Elahi E, Ali Z, Jamshaid H, Zeb A, Nadeem T, Ahmed W and Khan S (2022). Levosulpiride-loaded nanostructured lipid carriers for brain delivery with antipsychotic and antidepressant effects. Life Sci, 311: 121198.

Mehnert W and Mäder KJ (2012). Solid lipid nanoparticles: Production, characterization and applications. Adv Drug Deliv Rev, 64: 83-101.

Metz M and Ständer S (2010). Chronic pruritus–pathogenesis, clinical aspects and treatment. Journal of the European Academy of Dermatology and Venereology. J Eur Acad Dermatol, 24 (11): 1249-1260.

Misal G, Dixit G and Gulkari V (2012). Formulation and evaluation of herbal gel. Indian J Nat Prod Resour, 3: 501-504.

Mollanazar NK, Koch SD and Yosipovitch G (2015). Epidemiology of chronic pruritus: Where have we been and where are we going? Current dermatology reports. Curr Derm Rep, 4: 20-29.

Moulik SP, Paul BKJAiC and science I (1998). Structure, dynamics and transport properties of microemulsions. 78 (2): 99-195.

Patel T and Yosipovitch G (2010). Therapy of pruritus. Expert Opin Pharmacother, 11 (10): 1673-82.

Pereira MP and Ständer S (2017). Assessment of severity and burden of pruritus. Allergol Intern, 66 (1): 3-7.

Pradhan M, Singh D, Murthy SN and Singh MR (2015). Design, characterization and skin permeating potential of fluocinolone acetonide loaded nanostructured lipid carriers for topical treatment of psoriasis. Steroids, 101: 56-63.

Prignano F, Ricceri F, Pescitelli L and Lotti T (2009). Itch in psoriasis: Epidemiology, clinical aspects and treatment options. Clin Cosmet Investig Dermatol, 19: 9-13.

Rabia S, Khaleeq N, Batool S, Dar MJ, Kim DW, Din F-U and Khan GM (2020). Rifampicin-loaded nanotransferosomal gel for treatment of cutaneous leishmaniasis: Passive targeting via topical route. Int J Nanomed, 15 (2): 183-203.

Rashidi Nodeh H, Wan Ibrahim WA, Ali I, Sanagi M and Research P (2016). Development of magnetic graphene oxide adsorbent for the removal and preconcentration of as (iii) and as (v) species from environmental water samples. Environ Sci Pollut, 23 9759-9773.

Reich A, Ständer S and Szepietowski (2011). Pruritus in the elderly. Clin Dermatoll, 29 (1): 15-23.

Sabir F, Asad MI, Qindeel M, Afzal I, Dar MJ, Shah KU, Zeb A, Khan GM, Ahmed N and Din FU (2019). Polymeric nanogels as versatile nanoplatforms for biomedical applications. Clin Dermatol, 29:15-23.

Sanad RA, AbdelMalak NS, Elbayoomy TS and Badawi AP (2010). Formulation of a novel oxybenzone-loaded nanostructured lipid carriers (nlcs). AAPS Pharm Sci Tech, 11: 1684-1694.

Savoji H, Godau B, Hassani MS and Akbari M (2018). Skin tissue substitutes and biomaterial risk assessment and testing. Front Bioeng Biotechnol, 6(2): 112-119.

Sharma A, Upadhyay DK, Sarma GS, Kaur N, Gupta GD, Narang RK, Rai VK and Technology (2020). Squalene integrated nlc based gel of tamoxifen citrate for efficient treatment of psoriasis: . J Drug Deliv Sci Technol, 56: 509-568.

Ständer S, Steinhoff M, Schmelz M, Weisshaar E, Metze D and Luger T (2003). Neurophysiology of pruritus: Cutaneous elicitation of itch. Arch Dermatol, 139 (11): 1463-1470.

Stimmel GL, Dopheide JA and Stahl SM (1997). Mirtazapine: An antidepressant with noradrenergic and specific serotonergic effects. Pharmacotherapy: J hum Clin Pharmacol Ther, 17 (1): 10-21.

Suksaeree J, Treelop A, Veeravatanayothin P, Maneewattanapinyo P and Monton C. Stability test of nanostructured lipid carriers-loaded mefenamic acid prepared by microemulsion technique. IOP Conference Series: Mater Sci Eng, 840: 12001. IOP publishing, 012001.

Taylor JS, Zirwas MJ and Sood A (2010). Definition and etiology. Current Clinical Medicine E-Book: Expert Consult-Online, 13: 305.

Thomas S, Soloman P and Rejini VJ (2016). Preparation of chitosan-cmc blends and studies on thermal properties. Int Conf Eng Sci Tech, 24: 721-726.

Waghule T, Rapalli VK, Gorantla S, Saha RN, Dubey SK, Puri A and Singhvi (2020). Nanostructured lipid carriers as potential drug delivery systems for skin disorders. Curr Parm Des, 26 (36): 4569-4579.

Weisshaar E, Kucenic MJ and Fleischer Jr AB (2003). Pruritis A review. Acta Derm Venereol, 2: 83

Wong L-S, Yen Y-T and Lee C-H (2021). The implications of pruritogens in the pathogenesis of atopic dermatitis. Int J Mol Sci , 22 (13): 7227.

Yoon G, Park JW and Yoon IS (2013). Solid lipid nanoparticles (slns) and nanostructured lipid carriers (nlcs). Adv Drug Deliv, 43: 353-362.

Annexure I: Approval from Bioethics Committee.

قائداعظم یونیورسٹی
QUAID-I-AZAM UNIVERSITY
Faculty of Biological Sciences
Bioethics Committee

No. #BEC-FBS-QAU2022-440 Dated: 18-10-2022

Mr. Muhammad Akhtar
C/O Dr. Ahmad Khan,
Department of Pharmacy,
Faculty of Biological Sciences,
Quaid-i-Azam University, Islamabad
45320, Pakistan

Subject: - **"Preparation, optimization and characterization of Mirtazapine-loaded NLCs for treatment of Pruritus."**

Dear Mr. Muhammad Akhtar,

We wish to inform you that your subject research study has been reviewed and is hereby granted approval for implementation by Bio-Ethical Committee (BEC) of Quaid-i-Azam University. Your study has been assigned protocol **#BEC-FBS-QAU2022-440.**

While the study is in progress, please inform us of any adverse events or new, relevant information about risks associated with the research. In case changes have to be made to the study procedure, the informed consent from and or informed consent process, the BEC must review and approve any of these changes prior to implementation.

Sincerely,

Prof. Dr. Sarwat Jahan
Department of Zoology

cc:
Dean, F.B.S

Annexure II: Turnitin Similarity Index Report

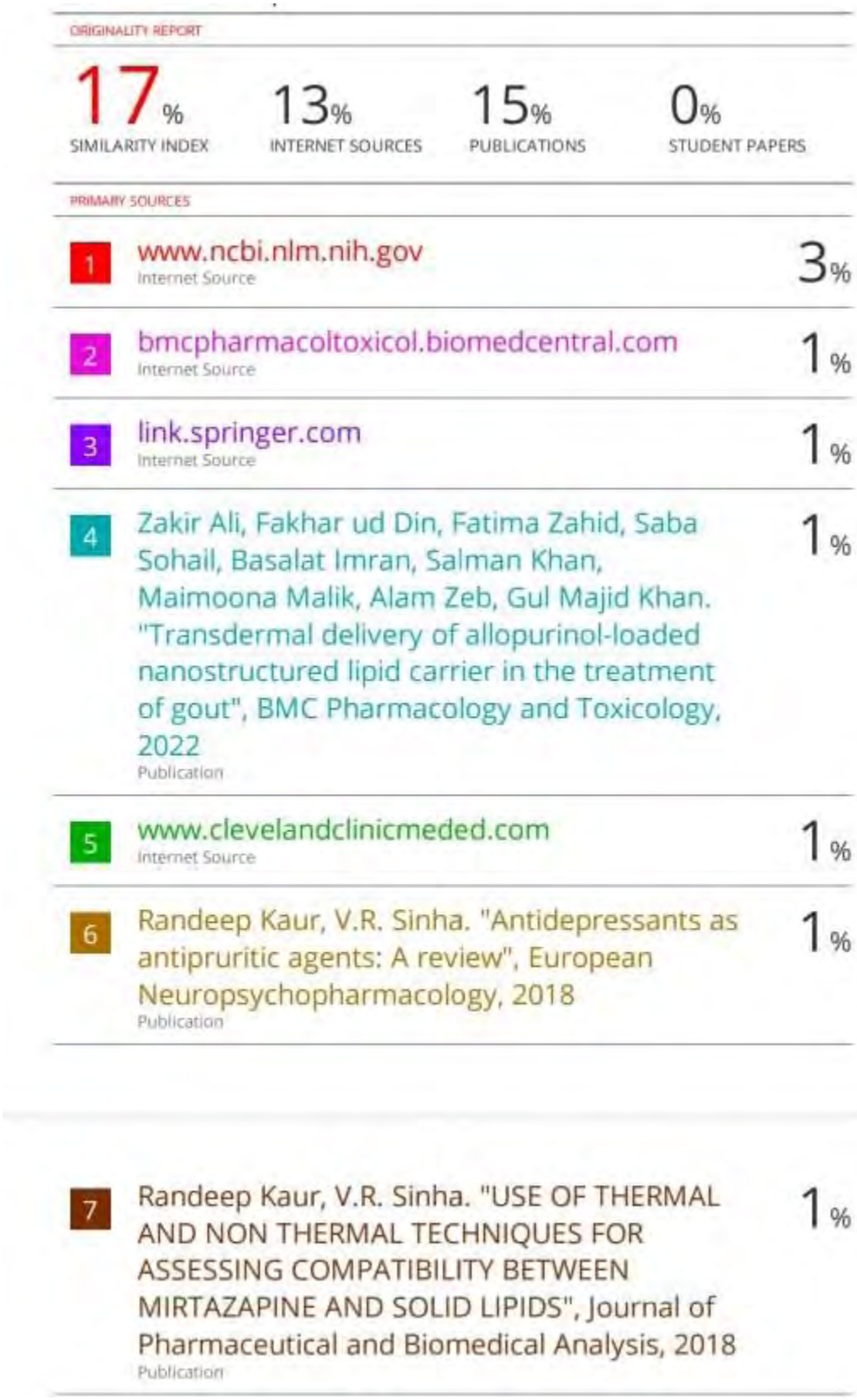

ORIGINALITY REPORT

17%	13%	15%	0%
SIMILARITY INDEX	INTERNET SOURCES	PUBLICATIONS	STUDENT PAPERS

PRIMARY SOURCES

1	www.ncbi.nlm.nih.gov Internet Source	3%
2	bmcpharmacoltoxicol.biomedcentral.com Internet Source	1%
3	link.springer.com Internet Source	1%
4	Zakir Ali, Fakhar ud Din, Fatima Zahid, Saba Sohail, Basalat Imran, Salman Khan, Maimoona Malik, Alam Zeb, Gul Majid Khan. "Transdermal delivery of allopurinol-loaded nanostructured lipid carrier in the treatment of gout", BMC Pharmacology and Toxicology, 2022 Publication	1%
5	www.clevelandclinicmeded.com Internet Source	1%
6	Randeep Kaur, V.R. Sinha. "Antidepressants as antipruritic agents: A review", European Neuropsychopharmacology, 2018 Publication	1%
7	Randeep Kaur, V.R. Sinha. "USE OF THERMAL AND NON THERMAL TECHNIQUES FOR ASSESSING COMPATIBILITY BETWEEN MIRTAZAPINE AND SOLID LIPIDS", Journal of Pharmaceutical and Biomedical Analysis, 2018 Publication	1%